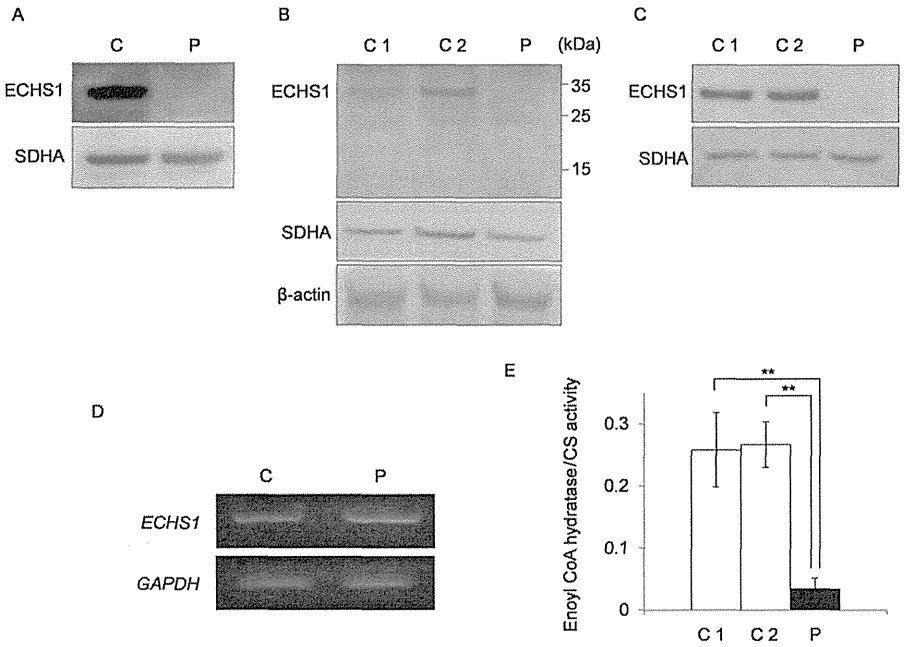


**Figure 3.** ECHS1 expression and enzyme activity. ECHS1 expression was analyzed by immunoblotting. C1/2, control; P, patient. Mitochondrial fraction prepared from patient's skeletal muscle (**A**) or whole-cell lysate (**B**) and mitochondrial fraction (**C**) prepared from the patient-derived myoblasts were analyzed via immunoblotting. All findings indicated that ECHS1 levels in patient samples were too low to detect by immunoblotting. **D**: RT-PCR was used to assess *ECHS1* mRNA levels in the patient. Notably, patient-derived myoblasts and control myoblasts did not differ with regard to *ECHS1* mRNA level. **E**: Mitochondrial fractions prepared from patient-derived myoblasts were used to estimate ECHS1 enzyme activity in the patient. All ECHS1 activity measurements were normalized to CS activity; ECHS1 activity in patient-derived samples was 13% of that in control samples. The experiments were performed in triplicate. Error bars represent standard deviations. (** $P < 0.005$ Student's *t*-test).

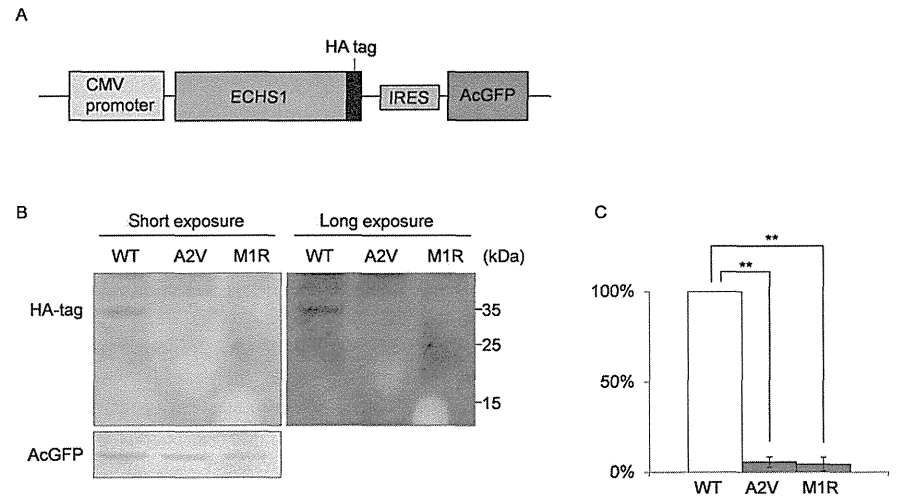


**Figure 4.** Exogenous expression of mutant ECHS1 protein in cancer cells. **A**: Schematic diagram of the pIRES mammalian expression vector. **B**: Representative image of an immunoblotting containing AcGFP, an internal control, and each HA-tagged ECHS1 protein; all proteins were isolated from DLD-1 cells that transiently overexpressed wild-type, A2V, or M1R HA-tagged ECHS1 from pIRES. The images obtained by short exposure (left) and long exposure (right). **C**: Overexpressed HA-tagged ECHS1 protein levels. Both mutant ECHS1 proteins showed dramatically decreased expression compared to wild-type ECHS1 protein, when ECHS1 was normalized relative to the internal control. Each experiment was performed in triplicate. Error bars represent standard deviations (** $P < 0.005$ Student's *t*-test).

## Discussion

Here, we described a patient harboring compound heterozygous mutations in *ECHS1*. Immunoblotting analysis revealed that ECHS1 protein was undetectable in patient-derived myoblasts; moreover, these cells showed significantly lower ECHS1 enzyme activity than controls. Exogenous expression of two recombinant mutant proteins in DLD-1 cells showed c.2T>G; p.M1R and c.5C>T; p.A2V mutations affected ECHS1 protein expression. Cellular complementation experiment verified the patient had ECHS1 deficiency.

The c.2T>G; p.M1R mutation affected the start codon and therefore was predicted to impair the protein synthesis from canonical

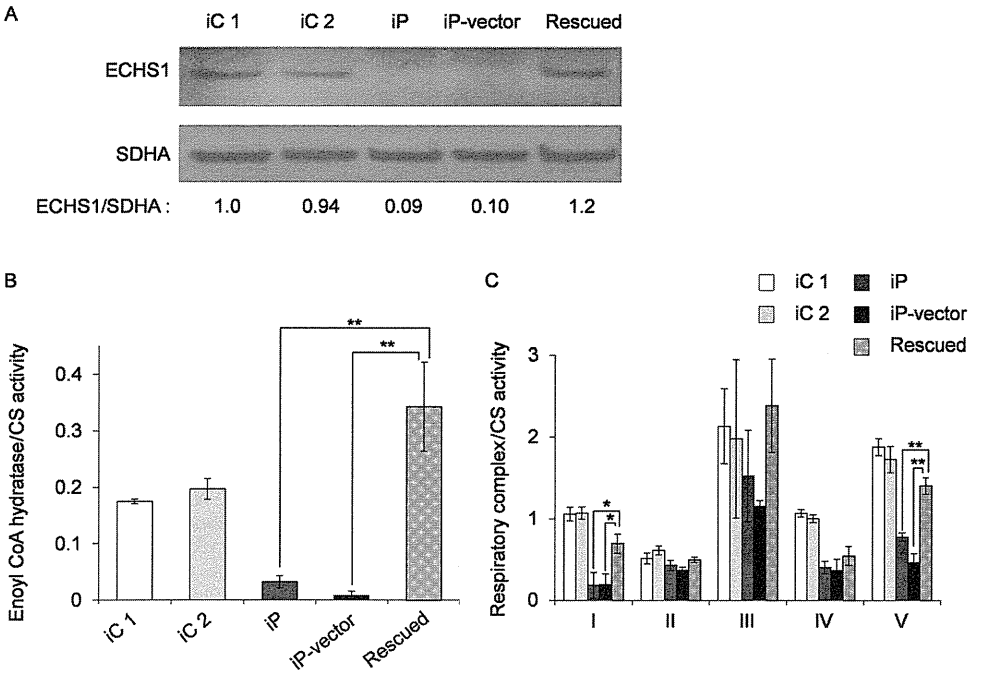


**Figure 5.** ECHS1 protein expression and enzyme activity in rescued myoblasts. An empty vector or a construct encoding wild-type ECHS1 was introduced into immortalized patient-derived myoblasts. iC1/2, immortalized control myoblasts; iP, immortalized patient-derived myoblasts; iP-vector, immortalized patient-derived myoblasts transfected with empty vector; Rescued, immortalized patient-derived myoblasts stably expressing wild-type ECHS1. **A**: ECHS1 levels were assessed on immunoblotting using mitochondrial fractions prepared from rescued myoblasts. ECHS1 level in "rescued" is 11 times higher than that in "iP-vector". **B**: Mitochondrial fractions prepared from rescued myoblasts were also used to measure ECHS1 enzyme activity. ECHS1 activity normalized to CS activity in "rescued" was 49 times higher than that in "iP-vector." Each experiment was performed in triplicate. Error bars represent standard deviations (** $P < 0.005$ Student's *t*-test). **C**: Mitochondrial fractions prepared from rescued myoblasts were used to measure enzyme activities of mitochondrial respiratory complexes. Activity values were normalized to CS activity. Activities of complexes I, IV, and V were mostly restored from "iP" and "iP-vector." In "rescued," the enzyme activities of complexes I, IV, and V were 3.5, 1.3, and 2.2 times higher, respectively, than the "iP-vector." Each experiment was performed in triplicate. Error bars represent standard deviations (** $P < 0.005$, * $P < 0.05$ Student's *t*-test).

initiation site. In the reference *ECHS1* sequence, the next in-frame start codon is located in amino acids 97 (Fig. 2C). Even if translation could occur from this second start codon, the resulting product would lack the whole transit peptide and part of the enoyl-CoA hydratase/isomerase family domain (Fig. 2C). The c.5C>T; p.A2V mutation was located in the mitochondrial transit peptide and the mutation may affect the mitochondrial translocation of ECHS1. Surprisingly, the MitoProt-predicted mitochondrial targeting scores for the wild-type and A2V-mutant proteins were 0.988 and 0.991, respectively [MitoProt II; http://ihg.gsf.de/ihg/mitoprot.html; Claros and Vincens, 1996] and not markedly different from each other. Nevertheless, mislocalized mutant protein may have been degraded outside of the mitochondria. Consistent with this speculation was the finding that immunoblotting of lysate from patient-derived myoblasts (Fig. 3B) or from transfected cells that overexpressed the recombinant p.A2V-mutant ECHS1 (Fig. 4B, Supp. Fig. S2) did not show upper shifted ECHS1 bands that indicated ECHS1 with the transit peptide. Another possible explanation is that the mutation affected the translation efficiency because it was very close to the canonical start codon. It can change secondary structure of ECHS1 mRNA or alter the recognition by the translation initiation factors. As stated above, even if there was a translation product from the second in-frame start codon, that product would probably not function.

This patient presented with symptoms that are indicative of fatty acid oxidation disorders (e.g., hypotonia and metabolic acidosis), but he also presented with neurologic manifestations, including developmental delay and Leigh syndrome, that are not normally associated with fatty acid $\beta$-oxidation disorders. Interestingly, developmental delay is also found in cases of SCAD deficiency [Jethva et al., 2008]. In the absence of SCAD, the byproducts of butyryl-CoA—including butyrylcarnitine, butyrylglycine, ethylmalonic acid (EMA), and methylsuccinic acid—accumulate in blood, urine, and cells. These byproducts may cause the neurological pathology associated with SCAD deficiency [Jethva et al., 2008]. EMA significantly inhibits creatine kinase activity in the cerebral cortex of Wistar rats but does not affect levels in skeletal or heart muscle [Corydon et al., 1996]. Elevated levels of butyric acid modulated gene expression because excess butyric acid can enhance histone deacetylase activity [Chen et al., 2003]. Moreover, the highly volatile nature of butyric acid as a free acid may also add to its neurotoxic effects [Jethva et al., 2008].

On the other hand, it is very rare for fatty acid $\beta$-oxidation disorders causing Leigh syndrome. Therefore, the most noteworthy manifestation in this patient was Leigh syndrome. Leigh syndrome is a neuropathological entity characterized by symmetrical necrotic lesions along the brainstem, diencephalon, and basal ganglion [Leigh, 1951]. It is caused by abnormalities of mitochondrial energy generation and exhibits considerable clinical and genetic heterogeneity [Chol et al., 2003]. Commonly, defects in the mitochondrial respiratory chain or the pyruvate dehydrogenase complex are responsible for this disease. This patient's skeletal muscle samples exhibited a combined respiratory chain deficiency, and this deficiency may be the reason that he presented with Leigh syndrome. Although it

remained unclear what caused the respiratory chain defect, cellular complementation experiments showed almost complete restoration, indicating there was an unidentified link between ECHS1 and respiratory chain. One of the possible causes of respiratory chain defect is the secondary effect of accumulation of toxic metabolites. For example, an elevated urine glyoxylate was observed in this patient. Although the mechanism of this abnormal accumulation is not clear at the moment, it was shown that glyoxylate inhibited oxidative phosphorylation or pyruvate dehydrogenase complex by in vitro systems [Whitehouse et al., 1974; Lucas and Pons, 1975]. Therefore, we speculate that in our patient, ECHS1 deficiency induced metabolism abnormality including glyoxylate accumulation, and glyoxylate played a role in decreased enzyme activities of respiratory chain complexes. Interestingly, a recent paper describing patients with Leigh syndrome and ECHS1 deficiency showed decreased activity of pyruvate dehydrogenase complex in fibroblasts [Peters et al., 2014], (Supp. Table S5). BN-PAGE showed the assembly of respiratory complex components in the patient was not clearly different from the control (Supp. Fig. S1). This result suggests that the respiratory chain defect in the patient is more likely because of the secondary effect of accumulation of toxic metabolites. On the other hand, many findings indicate interplays between mitochondrial fatty acid $\beta$-oxidation and the respiratory chain. For example, Enns et al. [2000] mentioned the possibility of the physical association between these two energy-generating pathways from overlapping clinical phenotypes in genetic deficiency states. More recently, Wang and his colleagues actually showed physical association between mitochondrial fatty acid $\beta$-oxidation enzymes and respiratory chain complexes (Wang et al., 2010). Similarly, Narayan et al. demonstrated interactions between short-chain 3-hydroxyacyl-CoA dehydrogenase (SCHAD) and several components of the respiratory chain complexes including the catalytic subunits of complexes I, II, III, and IV via pull-down assays involving several mouse tissues. Considering the role of SCHAD as a NADH-generating enzyme, this interaction was suggested to demonstrate the logical physical association with the regeneration of NAD through the respiratory chain [Narayan et al., 2012]. Still more recently, mitochondrial protein acetylation was found to be driven by acetyl-CoA produced from mitochondrial fatty acid $\beta$-oxidation [Pougovkina et al., 2014]. Because the activities of respiratory chain enzymes are regulated by protein acetylation [Zhang et al., 2012], this finding indicated that $\beta$-oxidation regulates the mitochondrial respiratory chain. Remarkably, acyl-CoA dehydrogenase 9 (ACAD9), which participates in the oxidation of unsaturated fatty acid, was recently identified as a factor involved in complex I biogenesis [Haack et al., 2010; Heide et al., 2012]. Cellular complementation experiments that involve overexpression of wild-type ACAD9 in patient-derived fibroblast cell lines showed restoration of complex I assembly and activity [Haack et al., 2010]. Accumulating evidence indicates that there are complex regulatory interactions between mitochondrial fatty acid $\beta$-oxidation and the respiratory chain.

ECHS1 has been shown to interact with several molecules outside the mitochondrial fatty acid $\beta$-oxidation pathway [Chang et al., 2013; Xiao et al., 2013] and the loss of this interaction can affect respiratory chain function in a patient. Further functional analysis of ECHS1 will advance our understanding of the complex regulation of mitochondrial metabolism.

## Acknowledgments

We acknowledge the technical support of Dr. Ichizo Nishino, Dr. Ikuya Nonaka, Dr. Chikako Waga, Takao Uchiumi, Yoshie Sawano, and Michiyo Nakamura. We also thank Dr. Sumio Sugano (the University of Tokyo) for providing the pEF321-T plasmid.

*Disclosure statement*: The authors have no conflict of interest to declare.

## References

Chang Y, Wang SX, Wang YB, Zhou J, Li WH, Wang N, Fang DF, Li HY, Li AL, Zhang XM, Zhang WN. 2013. ECHS1 interacts with STAT3 and negatively regulates STAT3 signaling. FEBS Lett 587:607–613.

Chen JS, Faller DV, Spanjaard RA. 2003. Short-chain fatty acid inhibitors of histone deacetylases: promising anticancer therapeutics? Curr Cancer Drug Targets 3:219–236.

Chol M, Lebon S, Bénit P, Chretien D, de Lonlay P, Goldenberg A, Odent S, Hertz-Pannier L, Vincent-Delorme C, Cormier-Daire V, Rustin P, Rötig A, et al. 2003. The mitochondrial DNA G13513A MELAS mutation in the NADH dehydrogenase 5 gene is a frequent cause of Leigh-like syndrome with isolated complex I deficiency. J Med Genet 40:188–191.

Claros MG, Vincens P. 1996. Computational method to predict mitochondrially imported proteins and their targeting sequences. Eur J Biochem 241:779–786.

Corydon MJ, Gregersen N, Lehnert W, Ribes A, Rinaldo P, Kmoch S, Christensen E, Kristensen TJ, Andresen BS, Bross P, Winter V, Martinez G, et al. 1996. Ethylmalonic aciduria is associated with an amino acid variant of short chain acyl-coenzyme A dehydrogenase. Pediatr Res 39:1059–1066.

Enns GM, Bennett MJ, Hoppel CL, Goodman SI, Weisiger K, Ohnstad C, Golabi M, Packman S. 2000. Mitochondrial respiratory chain complex I deficiency with clinical and biochemical features of long-chain 3-hydroxyacyl-coenzyme A dehydrogenase deficiency. J Pediatr 136:251–254.

Ensenauer R, He M, Willard JM, Goetzman ES, Corydon TJ, Vandahl BB, Mohsen A-W, Isaya G, Vockley J. 2005. Human acyl-CoA dehydrogenase-9 plays a novel role in the mitochondrial beta-oxidation of unsaturated fatty acids. J Biol Chem 280:32309–32016.

Frezza C, Cipolat S, Scorrano L. 2007. Organelle isolation: functional mitochondria from mouse liver, muscle and cultured filroblasts. Nat Protoc 2:287–295.

Haack TB, Danhauser K, Haberberger B, Hoser J, Strecker V, Boehm D, Uziel G, Lamantea E, Invernizzi F, Poulton J, Rolinski B, Iuso A, et al. 2010. Exome sequencing identifies ACAD9 mutations as a cause of complex I deficiency. Nat Genet 42:1131–1134.

Heide H, Bleier L, Steger M, Ackermann J, Dröse S, Schwamb B, Zörnig M, Reichert AS, Koch I, Wittig I, Brandt U. 2012. Complexome profiling identifies TMEM126B as a component of the mitochondrial complex I assembly complex. Cell Metab 6:538–549.

Hochstrasser DF, Frutiger S, Paquet N, Bairoch A, Ravier F, Pasquali C, Sanchez JC, Tissot JD, Bjellqvist B, Vargas R, Ron DA, Graham JH. 1992. Human liver protein map: a reference database established by microsequencing and gel comparison. Electrophoresis 13:992–1001.

Ikeda Y, Dabrowski C, Tanaka K. 1983. Separation and properties of five distinct acyl-CoA dehydrogenases from rat liver mitochondria. J Biol Chem 258:1066–1076.

Ikeda Y, Hine DG, Okamura-Ikeda K, Tanaka K. 1985a. Mechanism of action of short-chain, medium chain and long-chain acyl-CoA dehydrogenases: direct evidence for carbanion formation as an intermediate step using enzyme-catalyzed C-2 proton/deuteron exchange in the absence of C-3 exchange. J Biol Chem 260: 1326–1337.

Ikeda Y, Okamura-Ikeda K, Tanaka K. 1985b. Spectroscopic analysis of the interaction of rat liver short chain, medium chain and long chain acyl-CoA dehydrogenases with acyl-CoA substrates. Biochemistry 24:7192–7199.

Jethva R, Bennett MJ, Vockley J. 2008. Short-chain acyl-coenzyme A dehydrogenase deficiency. Mol Genet Metab 95:195–200.

Kamijo T, Aoyama T, Miyazaki J, Hashimoto T. 1993. Molecular cloning of the cDNAs for the subunits of rat mitochondrial fatty acid beta-oxidation multienzyme complex. Structural and functional relationships to other mitochondrial and peroxisomal beta-oxidation enzymes. J Biol Chem 268:26452–26460.

Kim DW, Uetsuki T, Kaziro Y, Yamaguchi N, Sugano S. 1990. Use of the human elongation factor 1 alpha promoter as a versatile and efficient expression system. Gene 91:217–223.

Kompare M, Rizzo WB. 2008. Mitochondrial fatty-acid oxidation disorders. Semin Pediatr Neurol 15:140–149.

Leigh D. 1951. Subacute necrotizing encephalomyelopathy in an infant. J Neurol Neurosurg Psychiatr 14:216–221.

Lucas M, Pons AM. 1975. Influence of glyoxylic acid on properties of isolated mitochondria. Biochimie 57:637–645.

Matsunaga T, Kumanomido H, Shiroma M, Goto Y, Usami S. 2005. Audiological features and mitochondrial DNA sequence in a large family carrying mitochondrial A1555G mutation without use of aminoglycoside. Ann Otol Rhinol Laryngol 114:153–160.

Morava E, Rodenburg RJ, Hol F, de Vries M, Janssen A, van den Heuvel L, Nijtmans L, Smeitink J. 2006. Clinical and biochemical characteristics in patients with a high mutant load of the mitochondrial T8993G/C mutations. Am J Med Genet A 140:863–868.

Narayan, SB, Master SR, Sirec AN, Bierl C, Stanley PE, Li C, Stanley CA, Bennett MJ. 2012. Short-chain 3-hydroxyacyl-coenzyme A dehydrogenase associates with a protein super-complex integrating multiple metabolic pathways. PLoS One 7: e35048.

Peters H, Buck N, Wanders R, Ruiter J, Waterham H, Koster J, Yaplito-Lee J, Ferdinandusse S, Pitt J. 2014. ECHS1 mutations in Leigh disease: a new inborn error of metabolism affecting valine metabolism. Brain 137: 2903–2908.

Pougovkina O, Te Brinke H, Ofman R, van Cruchten AG, Kulik W, Wanders RJ, Houten SM, de Boer VC. 2014. Mitochondrial protein acetylation is driven by acetyl-CoA from fatty acid oxidation. Hum Mol Genet 23:3513–3522.

Shimazaki H, Takiyama Y, Ishiura H, Sakai C, Matsushima Y, Hatakeyama H, Honda J, Sakoe K, Naoi T, Namekawa M, Fukuda Y, Takahashi Y, et al. 2012. A homozygous mutation of C12orf65 causes spastic paraplegia with optic atrophy and neuropathy (SPG55). J Med Genet 49:777–784.

Spiekerkoetter U, Khuchua Z, Yue Z, Bennett MJ, Strauss AW. 2004. General mitochondrial trifunctional protein (TFP) deficiency as a result of either alpha- or beta-subunit mutations exhibits similar phenotypes because mutations in either subunit alter TFP complex expression and subunit turnover. Pediatr Res 55:190–196.

Steinman HM, Hill RL. 1975. Bovine liver crotonase (enoyl coenzyme A hydratase). Methods Enzymol 35:136–151.

Uchida Y, Izai K, Orii T, Hashimoto T. 1992. Novel fatty acid beta-oxidation enzymes in rat liver mitochondria. II. Purification and properties of enoyl-coenzyme A (CoA) hydratase/3-hydroxyacyl-CoA dehydrogenase/3-ketoacyl-CoA thiolase trifunctional protein. J Biol Chem 267:1034–1041.

Wang Y, Mohsen AW, Mihalik SJ, Goetzman ES, Vockley J. 2010. Evidence for physical association of mitochondrial fatty acid oxidation and oxidative phosphorylation complexes. J Biol Chem 285:29834–29841.

Whitehouse S, Cooper RH, Randle PJ. 1974. Mechanism of activation of pyruvate dehydrogenase by dichloroacetate and other halogenated carboxylic acids. Biochem J 141:761–774.

Xiao CX, Yang XN, Huang QW, Zhang YQ, Lin BY, Liu JJ, Liu YP, Jazag A, Guleng B, Ren JL. 2013. ECHS1 acts as a novel HBsAg-binding protein enhancing apoptosis through the mitochondrial pathway in HepG2 cells. Cancer Lett 330:67–73.

Zhang J, Lin A, Powers J, Lam MP, Lotz C, Liem D, Lau E, Wang D, Deng N, Korge P, Zong, NC, Cai H, et al. 2012. Perspectives on: SGP symposium on mitochondrial physiology and medicine: mitochondrial proteome design: from molecular identity to pathophysiological regulation. J Gen Physiol 139:395–406.

*Exp. Anim. 63(4), 459–466, 2014*

—Original—

# Administration of an Antioxidant Prevents Lymphoma Development in Transmitochondrial Mice Overproducing Reactive Oxygen Species

Haruka YAMANASHI[1)†], Osamu HASHIZUME[2)†], Hiromichi YONEKAWA[3)], Kazuto NAKADA[2, 4, 5)], and Jun-Ichi HAYASHI[2, 4, 5)]

[1)]*Graduate School of Life and Environmental Sciences, University of Tsukuba, 1-1-1 Tennodai, Tsukuba, Ibaraki 305-8572, Japan*
[2)]*Faculty of Life and Environmental Sciences, University of Tsukuba, 1-1-1 Tennodai, Tsukuba, Ibaraki 305-8572, Japan*
[3)]*Center for Basic Technology Research, The Tokyo Metropolitan Institute of Medical Science, 2-1-6 Kamikitazawa, Setagaya-ku, Tokyo, 156-8506, Japan*
[4)]*International Institute for Integrative Sleep Medicine (WPI-IIIS), University of Tsukuba, 1-1-1 Tennodai, Tsukuba, Ibaraki 305-8575, Japan*
[5)]*Life Science Center of Tsukuba Advanced Research Alliance, University of Tsukuba, 1-1-1 Tennodai, Tsukuba, Ibaraki 305-8577, Japan*

**Abstract:** Because of the difficulty to exclude possible involvement of nuclear DNA mutations, it has been a controversial issue whether pathogenic mutations in mitochondrial DNA (mtDNA) and the resultant respiration defects are involved in tumor development. To address this issue, our previous study generated transmitochondrial mice (mito-mice-ND6$^{13997}$), which possess the nuclear and mtDNA backgrounds derived from C57BL/6J (B6) strain mice except that they carry B6 mtDNA with a G13997A mutation in the *mt-Nd6* gene. Because aged mito-mice-ND6$^{13997}$ simultaneously showed overproduction of reactive oxygen species (ROS) in bone marrow cells and high frequency of lymphoma development, current study examined the effects of administrating a ROS scavenger on the frequency of lymphoma development. We used *N*-acetylcysteine (NAC) as a ROS scavenger, and showed that NAC administration prevented lymphoma development. Moreover, its administration induced longevity in mito-mice-ND6$^{13997}$. The gene expression profiles in bone marrow cells indicated the upregulation of the *Fasl* gene, which can be suppressed by NAC administration. Given that natural-killer (NK) cells mediate the apoptosis of various tumor cells via enhanced expression of genes encoding apoptotic ligands including *Fasl* gene, its overexpression would reflect the frequent lymphoma development in bone marrow cells. These observations suggest that continuous administration of an antioxidant would be an effective therapeutics to prevent lymphoma development enhanced by ROS overproduction.
**Key words:** antioxidant, lymphoma prevention, mouse mtDNA mutation, ROS overproduction

## Introduction

Mitochondrial DNA (mtDNA) mutations that induce mitochondrial respiration defects have been proposed to be involved in aging and age-associated disorders including tumor development [13, 14, 18, 23, 24]. Moreover,

*(Received 1 May 2014 / Accepted 27 May 2014 / Published online in J-STAGE 22 July 2014)*
*Address corresponding: J. Hayashi, Faculty of Life and Environmental Sciences, University of Tsukuba, 1-1-1 Tennodai, Tsukuba, Ibaraki 305-8572, Japan*
† *These two authors contributed equally to this study.*

mitochondrial respiration defects caused by nuclear DNA mutations and the resultant enhanced glycolysis under normoxic conditions, i.e. the Warburg effect, are reported to be responsible for tumor development [4, 7, 16, 19]. Therefore, it is also possible that mitochondrial respiration defects caused by an age-associated accumulation of mtDNA mutations induce the Warburg effect via compensatory upregulation of aerobic glycolysis, resulting in tumor development. In fact, somatic mutations were preferentially accumulated in tumor mtDNA [6, 10, 21]. However, there has been no direct evidence for the involvement of mtDNA mutations in the Warburg effect and in tumor development, because of the difficulty to exclude possible involvement of nuclear DNA mutations in these processes [2].

Our previous studies [1, 11, 12] resolved this issue by the use of intercellular mtDNA transfer technology between mouse cells expressing different phenotypes related to tumors. While mtDNA introduced from tumor cells into normal cells did not induce tumorigenicity [1], mtDNA exchange between poorly and highly metastatic lung carcinoma cells provided convincing evidence that a somatic G13997A mtDNA mutation in the *mt-Nd6* gene, which encodes subunit 6 of respiration complex I (NADH dehydrogenase), reversibly controls development of highly metastatic potentials [11]. In this case, the induction of high metastasis was not due to the Warburg effect, but to overproduction of the reactive oxygen species (ROS) [12]. Subsequently, G13997A mtDNA was transferred from highly metastatic carcinoma cells into mouse female germ line [26] to examine the effect of the G13997A mtDNA on tumor-related phenotypes. The resultant transmitochondrial mice possessing only G13997A mtDNA, named mito-mice-ND6$^{13997}$, showed high frequently of lymphoma formation with aging [9], providing convincing evidence for the involvement of the mtDNA mutations in tumor development.

Based on these observations, this study examined whether continuous administration of an antioxidant prevents lymphoma development, and corresponds to an effective therapeutics to protect lymphoma development in mito-mice-ND6$^{13997}$. We also examined the mechanisms of how ROS induce lymphoma formation in mito-mice-ND6$^{13997}$.

## Materials and Methods

*Ethical statement*

All animal experiments were performed in accordance with protocols approved by the experimental animal committee of the University of Tsukuba, Japan.

*Mice*

Old inbred C57BL/6J Jcl (B6) mice were obtained from CLEA Japan. Mito-mice-ND6$^{13997}$ were generated in our previous work [26]. We maintained B6 mice and mito-mice-ND6$^{13997}$ sharing a common nuclear DNA background by repeated backcrossing of their females with B6 males. Animals were housed in groups of up to 5 in individually ventilated cages under standard conditions (22°C, 12 h light–dark cycle) receiving food and water *ad libitum*. Male mice were used in the experiments, and were monitored everyday for general health and signs of tumor burden such as hunched postures, ruffled coats and respiratory distress were humanely killed. Moribund mice were euthanized by cervical dislocation under general anesthesia (Avertin, 1.25%, 0.2 ml/20 g body weight, intraperitoneally).

*NAC administration*

At 15 months old, sixteen mito-mice-ND6$^{13997}$ were divided at random into two groups. One group was given drinking water containing 10 g/l of NAC (SIGMA), and another group was given regular water. NAC supplemented water and regular water were prepared fresh everyday.

*Histological analyses*

Formalin-fixed, paraffin-embedded serial sections (10 $\mu$m) were used for histological analyses. Hematoxylin-and-eosin–stained sections were used for histopathological analysis to identify tumor tissues. The immunohistological analysis was performed with antibody to CD45 to determine whether the tumor tissues originated from leukocytes, and subsequently with antibodies to B220 and CD3 to determine whether the tumor tissues were of B-cell or T-cell origin, respectively. Deparaffinized slides were boiled for antigen retrieval, then incubated with rat anti-mouse CD45 (clone 30-F11; BD Biosciences, Cat. No. 550539) at a dilution of 1:200 or rat anti-mouse B220 (clone RA3-6B2; BD Biosciences, Cat. No. 553085) at a dilution of 1:50 or goat anti-mouse CD3 (clone M-20; Santa Cruz, Cat. No. sc-1127) at a

dilution of 1:50. Biotin-conjugated goat anti-rat IgG (BD Biosciences, Cat. No. 559286) and rabbit anti-goat IgG (Vector Laboratories, Cat. No. BA-5000) were used as secondary antibody at a dilution of 1:50 and 1:500, respectively. Detection of CD45, B220 and CD3 were performed using avidin-biotin complex methodologies (Vectastain Elite ABC Kit, Vector Laboratories) with DAB staining (Anti-Ig HRP Detection Kit, BD Pharmingen). Sections were counterstained with hematoxylin.

*PCR array analysis*

Mice were euthanized after 4-week administration of NAC and bone marrow cells were isolated from mice thighbones and shinbones. Total RNA was extracted by ISOGEN (Nippon Gene) from mouse bone marrow cells. RNA samples were subjected to DNase I treatment (Invitrogen) to eliminate DNA contaminants and reverse transcribed using Oligo $(dT)_{12-18}$ primer, 10 mM dNTP Mix, 0.1 M DTT, RNase Out Recombinant Ribonuclease Inhibitor, and SuperScript II-Reverse Transcriptase (Invitrogen). cDNA samples were subjected to RNase H treatment (Invitrogen), and applied according to the manufacturer's protocol to a $RT^2$ profiler PCR array real-time PCR reaction. Real-time monitoring PCR was performed with SYBR Green PCR Master Mix (QIAGEN) and an ABI PRISM 7900HT sequence detection system (Applied Biosystems). Mouse Cancer Pathway Finder $RT^2$ Profiler PCR Array PAMM-033Z (SABiosciences) was performed to profile the expression of 84 genes related to the cancer pathway (n=3). The expression profiling was performed using ΔΔCt methods according to manufacturer's protocols. The relative expression level for each gene was represented as cycle threshold (Ct). Normalized expression level was calculated as ΔCt=Ct (Gene of interest) − Ct (control). The average ΔCt from three mice was calculated as the relative expression level of each gene. Differential expression was calculated as ΔΔCt=Ave ΔCt (sample mice) − Ave ΔCt (control mice). Fold change was calculated as $2^{-\Delta\Delta Ct}$. The *P* values are calculated based on a Student *t*-test of the replicate $2^{-\Delta Ct}$ values for each gene in the control group and treatment groups.

*Statistical analysis*

We analyzed data with the Student's *t*-test. Kaplan-Meier curves were assessed with the log-rank test. Values with $P<0.05$ were considered significant.

## Results

This study examined the idea that the frequent lymphoma development in the aged male mito-mice-ND6$^{13997}$ could be prevented by the administration of an antioxidant, if ROS overproduction is responsible for the lymphoma development. Since most mito-mice-ND6$^{13997}$ began to develop lymphoma more than 18 months after the birth [9], we used 15-month-old males for continuous administration of *N*-acetylcysteine (NAC) as a ROS scavenger. Eight of 16 mito-mice-ND6$^{13997}$ were treated with NAC from 15 months after the birth by oral administration based on the procedure reported previously [5]. The remaining eight mito-mice-ND6$^{13997}$ were not treated with NAC. Seven 15-month-old B6 males untreated with NAC were used as controls.

First, we examined whether the NAC treatment would affect the frequency of lymphoma development and the lifespan. Median survival times of NAC-treated mito-mice-ND6$^{13997}$, untreated mito-mice-ND6$^{13997}$ and untreated B6 mice were 29.3, 22.5 and 25.8 months, respectively (Figs. 1A and B). No statistical significance of median survival times was observed between untreated mito-mice-ND6$^{13997}$ and untreated B6 mice (Fig.1A). These results are consistent with our previous observations [9]. In contrast, NAC-treated mito-mice-ND6$^{13997}$ showed longer survival times than untreated mito-mice-ND6$^{13997}$ with statistical significance (Fig. 1B), while no statistical significance was present between NAC-treated mito-mice-ND6$^{13997}$ and untreated B6 mice (Figs. 1A and B). The median survival times of untreated mito-mice-ND6$^{13997}$ with and without lymphoma-like abnormalities were 24.5 and 20.5, respectively, and were not different with statistical significance (Fig. 1C).

Gross necropsy of all dead or euthanized moribund mice showed that three of eight mito-mice-ND6$^{13997}$(38%) and one of seven B6 mice (14%) had macroscopic lymphoma-like abnormalities, including enlarged spleen, liver, and nodular tumors, but none of eight NAC-treated mito-mice-ND6$^{13997}$ had these abnormalities (Table 1). Histological analyses of abnormal tissues revealed that all were hematopoietic neoplasms and positive for the pan-leukocyte marker CD45 (Table 1 and Fig. 2 ). These observations suggest that these hematological neoplasms may correspond to lymphoma cells, although current study did not examine copy-number variations (CNVs) in nuclear genomes to show chromosomal instability [9].

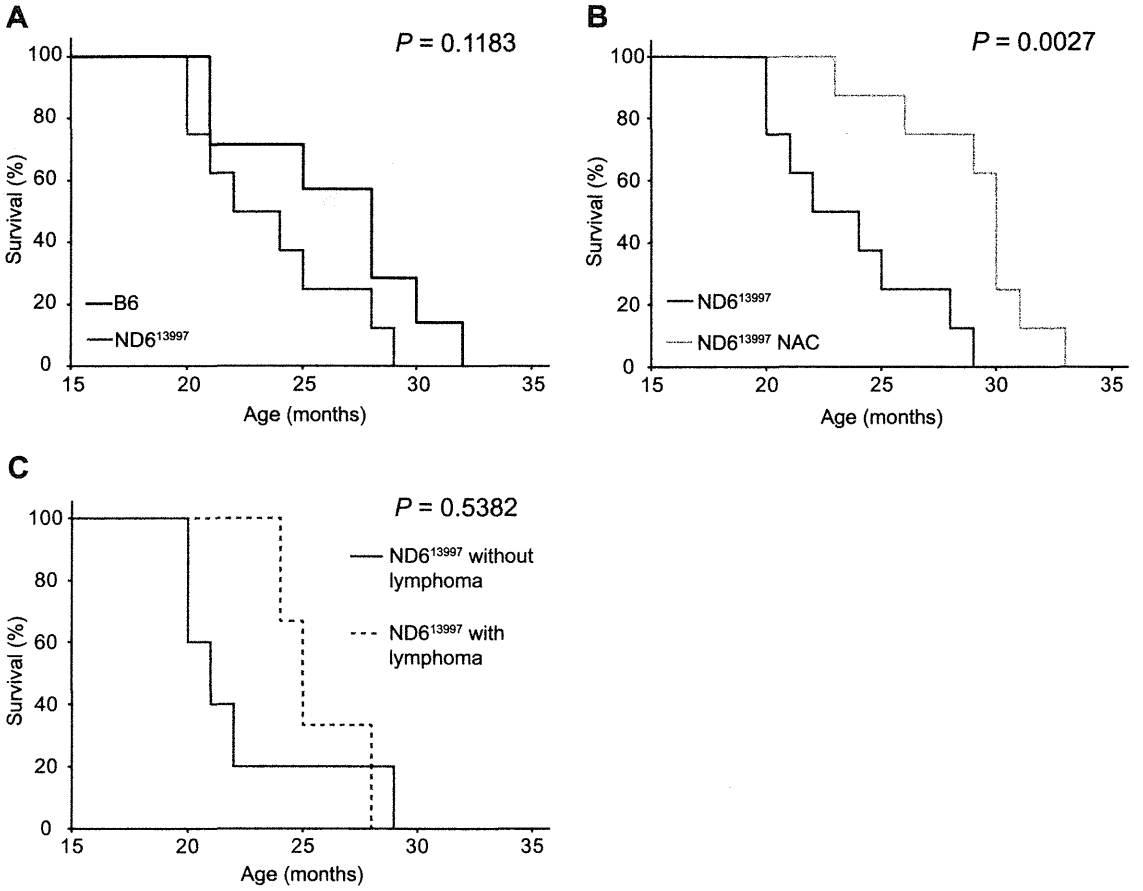


**Fig. 1.** Kaplan-Meier survival curves of mito-miceND6$^{13997}$. (A) Comparison of lifespans between B6 mice and mito-miceND6$^{13997}$. Median survival times of B6 mice (n=7) and mito-miceND6$^{13997}$(n=8) were 25.8 and 22.0 months, respectively. (B) Comparison of lifespans of between NAC-treated and untreated mito-miceND6$^{13997}$. NAC administration was started from 15 months after the birth to the end of their lives. Median survival times of mito-miceND6$^{13997}$(n=8) and mito-miceND6$^{13997}$ treated with NAC (n=8) were 22.0 and 29.3 months, respectively. (C) Comparison of lifespans between mito-miceND6$^{13997}$ that died with and without detectable lymphoma. Median survival times of mito-miceND6$^{13997}$ with detectable lymphoma (n=3) and mito-miceND6$^{13997}$ without detectable lymphoma (n=5) were 24.5 and 20.5 months, respectively.

**Table 1.** Frequencies of lymphoma development in mice

| Mouse strains | No. of mice | No. of mice with tumor | Tissues with tumor | | | Histological analysis | | | Cell lineage |
|---|---|---|---|---|---|---|---|---|---|
| | | | Spleen | Liver | Lymph node | CD45 | B220 | CD3 | |
| B6 | 7 | 1 | + | + | + | + | + | - | B-cell |
| Mito-mice-ND6$^{13997}$ | 8 | 3 | + | - | + | + | + | - | B-cell |
| | | | + | - | - | + | - | + | T-cell |
| | | | + | + | + | + | + | - | B-cell |
| Mito-mice-ND6$^{13997}$ (NAC-treated) | 8 | 0 | | | | | | | |

Three tumors were of B-cell origin, expressing the B-cell maker B220, while one mito-mouse-ND6$^{13997}$ developed T-cell lymphoma staining positive for the T-cell marker CD3 (Table 1). These data indicate that NAC administration is an effective therapeutics to prevent lymphoma development caused by ROS overproduction. However, further works using more numbers of animals than those used in this study are required to confirm this idea.

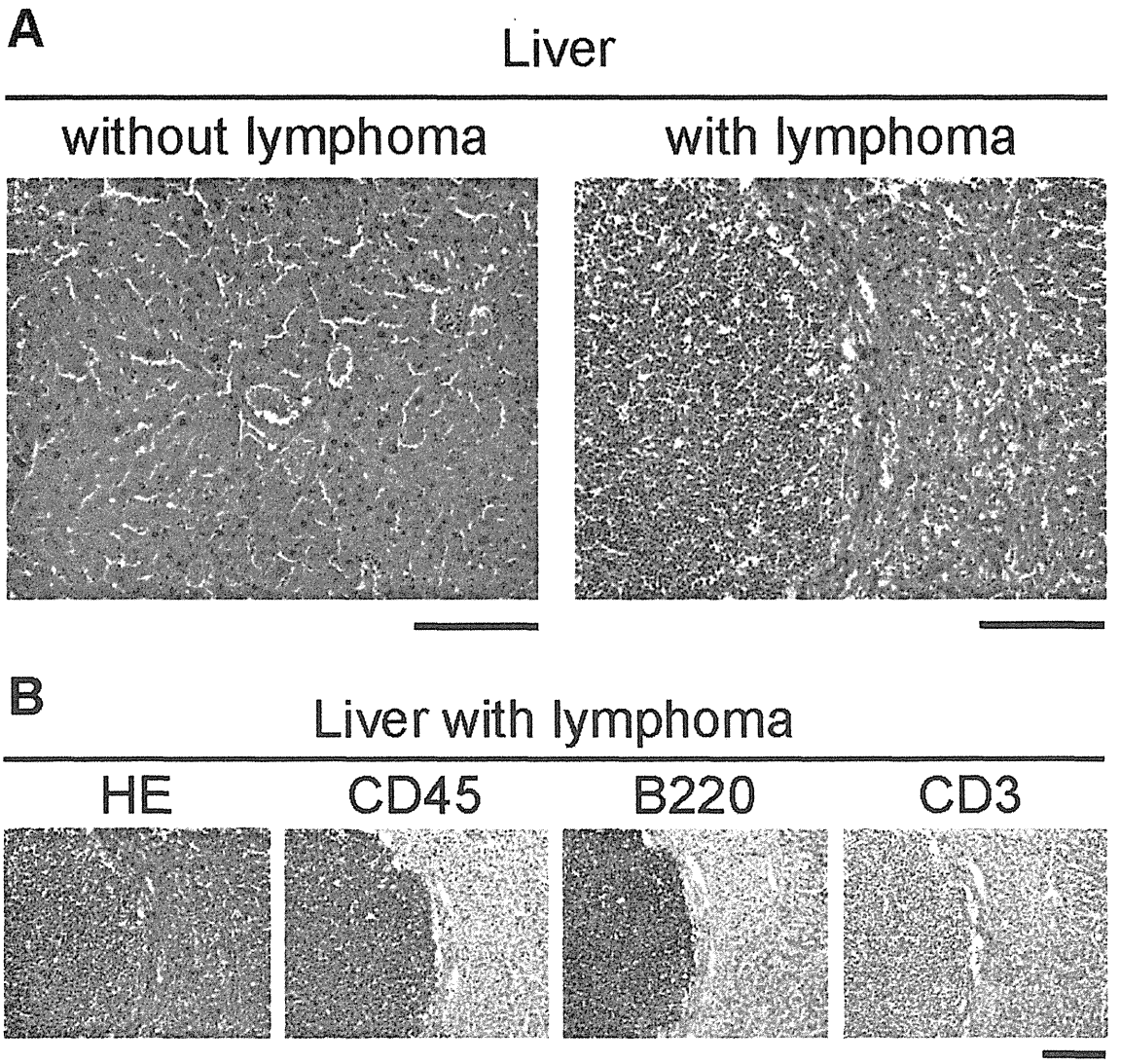


**Fig. 2.** Histological analyses for identification of lymphoma cells in the liver from mito-miceND6$^{13997}$. (A) Hematoxylin and eosin (HE) staining of the liver sections from mito-miceND6$^{13997}$. HE staining of the liver sections was carried out to identify tumor-like abnormalities in the liver. Left and right panels represent normal liver and liver with tumor-like abnormalities, respectively. (B) Histological analysis of serial sections of the liver with tumor-like abnormalities. HE, hematoxylin-eosin staining to show tumor formation; CD45, immunohistochemistry using antibody to CD45 to detect leukocytes; B220, immunohistochemistry using antibody to B220 to detect B cells; CD3, immunohistochemistry using antibody to CD3 to detect T cells. Because this tissue was stained positively with CD45 and B220, but not with CD3, the results represent abnormal growth of B cell-lymphoma, but not T cell-lymphoma, in the liver. (Scale bars, 200 $\mu$m).

Then, we examined the mechanism of frequent lymphoma development, which can be prevented by administration of an antioxidant to mito-mouse-ND6$^{13997}$. Our previous study showed that no tumors other than lymphoma were developed, and that ROS were overproduced in bone marrow cells but not in splenocytes [9]. It is therefore likely that the ROS overproduction in the bone marrow cells of mito-mouse-ND6$^{13997}$ is crucial for lymphoma development. Thus, we used bone marrow cells to identify genes that would be responsible for frequent lymphoma development in mito-mice-ND6$^{13997}$, and compared the expression of the genes related to cancer pathway (transformation and tumorigenesis) between mito-mice-ND6$^{13997}$ and B6 mice using PCR array (Mouse Cancer Pathway Finder RT$^2$ Profiler PCR Array). Because most mito-mice-ND6$^{13997}$ began to develop

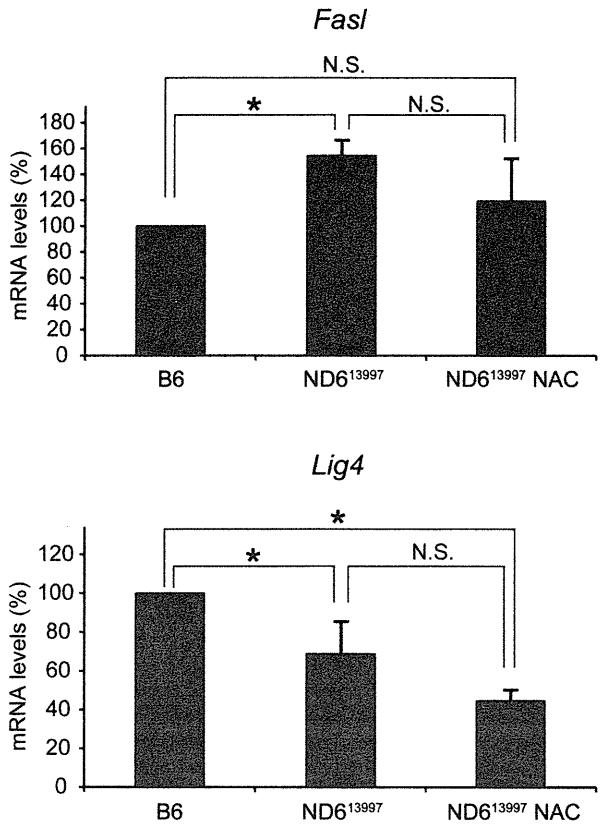


**Fig. 3.** Cancer related gene expression profiles of bone marrow cells. RT$^2$ Profiler mouse cancer pathway finder PCR array was performed on bone marrow cells. Two genes of 84 cancer pathway-related genes, *Fasl* and *Lig4*, were differentially expressed between bone marrow cells of B6 mice and mito-mice-ND6$^{13997}$. However, only the *Fasl* gene expression was reversibly regulated to normal levels by administration of NAC. Values were normalized to a pool of housekeeping genes on the array by ΔΔCt and are reported as the fold change in gene expression relative to healthy B6 bone marrow cells. Data are represented as mean values with SD (n=3). *, $P<0.05$.

lymphoma 18 months after the birth, we used 15-month-old male mice for this experiment to exclude the influence of the developed lymphoma cells.

Out of 84 cancer pathway-related genes represented on Mouse Cancer Pathway Finder RT$^2$ Profiler PCR Array (Supplemental table 1), only two genes, *Fasl* and *Lig4* related to apoptosis and DNA repair, respectively, were selected as genes being differentially expressed between bone marrow cells of B6 and mito-mice-ND6$^{13997}$(Fig. 3). Then, we examined whether expression levels of these genes can be changed to the levels of B6 mice by administration of NAC for 4 weeks to mito-mice-ND6$^{13997}$. The results showed that *Fasl* overexpression in mito-mice-ND6$^{13997}$ was suppressed to B6 levels by NAC administration, while suppressed expression of *Lig4* levels did not restore to B6 levels (Fig. 3). These results indicated the association of *Fasl* overexpression to frequent development of lymphoma in mito-mice-ND6$^{13997}$.

## Discussion

This study addressed two important issues of whether treatment of the mito-mice-ND6$^{13997}$ with an antioxidant could be an effective therapeutics to prevent lymphoma development mito-mice-ND6$^{13997}$, and how ROS overproduction caused by G13997A mtDNA introduced from highly metastatic lung carcinoma cells induces lymphoma development in mito-mice-ND6$^{13997}$.

Concerning the first issue on the therapeutics of lymphoma development, the results in this study showed that administration of NAC, one of the frequently used antioxidants, is very effective to prevent lymphoma development in mito-mice-ND6$^{13997}$. Our previous study proposed the idea that ROS overproduction, but not lactate overproduction, is responsible for frequent development of lymphoma in mito-mice-ND6$^{13997}$ with G13997A mtDNA based on the observations that lymphoma was not developed in different mito-mice-COI$^{6589}$ that showed lactate overproduction but did not show ROS overproduction [9]. If this idea is correct, it can be predicted that administration of the antioxidants would prevent lymphoma development in mito-mice-ND6$^{13997}$. Current study examined this prediction and showed that NAC administration is effective to prevent lymphoma development caused by ROS in mito-mice-ND6$^{13997}$. However, further works are required to show that NAC administration prevents ROS overproduction in bone marrow cells of mito-mice-ND6$^{13997}$.

While NAC administration prevents lymphoma development (Table 1), it also induced longevity in mito-mice-ND6$^{13997}$ (Fig. 1B). Median survival times of B6 mice, mito-mice-ND6$^{13997}$, and NAC-treated mito-mice-ND6$^{13997}$ were 25.8, 22.0, and 29.3, respectively (Figs. 1A and B). The longer median survival times of NAC-treated mito-mice-ND6$^{13997}$ would not be due to the prevention of lymphoma formation by NAC administration, because the median survival times of untreated mito-mice-ND6$^{13997}$ with and without lymphoma were 24.5 and 20.5, respectively, and were not different with statistical significance (Fig. 1C). Since it appears to be

controversial whether oxidative stress suppresses longevity or not [20, 25], we could not at present explain why NAC administration induced longevity in mito-mice-ND6$^{13997}$. To examine this issue, we have to carry out NAC administration not only to mito-mice-ND6$^{13997}$ but also to B6 mice using more numbers of animals.

Concerning the second issue of how ROS overproduction caused by G13997A mtDNA induced lymphoma development, this study showed that overexpression of *Fasl* is related the process, because its overexpression in mito-mice-ND6$^{13997}$ was suppressed to normal levels by NAC administration (Fig. 3). Given that natural-killer (NK) cells mediate the apoptosis of various tumor cells via the expression of genes encoding tumor necrosis factor-family ligands including the *Fasl* gene [22], it would not be conceivable that its overexpression is responsible for lymphoma development. Probably, overexpression of the *Fasl* gene in NK cells simply reflects the progress of the frequent lymphoma development in bone marrow cells of mito-mice-ND6$^{13997}$. Therefore, we could not at present explain the mechanisms of how ROS overproduction induces frequent lymphoma development in aged mito-mice-ND6$^{13997}$.

Then, a question is why mito-mice-ND6$^{13997}$ preferentially develop lymphoma [9] (Table 1), even though ROS induces various types of cellular damages, leading to genomic instability that can result in the development of various types of tumors [15]. One answer to this question would be that nuclear genetic background of B6 strain we used for generation of mito-mice-ND6$^{13997}$ is prone to develop lymphoma [3, 8, 17]. Based on these observations, we would like to propose an idea that G13997A mtDNA alone would not induce lymphoma development in the absence of B6 nuclear genetic background. To examine this idea, we are going to generate new mito-mice-ND6$^{13997}$ carrying G13997A mtDNA but carrying different nuclear genetic background derived from different mouse strains that are not prone to develop lymphoma by backcrossing female mito-mice-ND6$^{13997}$ to males from different mouse strains.

## Acknowledgments

This work was supported by Grants-in-Aid for Scientific Research A 25250011 (to J.-I.H.), Scientific Research A 23240058 (to K.N.), and Scientific Research on Innovative Areas 24117503 (to J.-I.H.) from the Japan Society for the Promotion of Science. This work was supported also by the World Premier International Research Center Initiative; Ministry of Education, Culture, Sports, Science and Technology–Japan (to K.N. and J.-I.H.).

## References

1. Akimoto, M., Niikura, M., Ichikawa, M., Yonekawa, H., Nakada, K., Honma, Y., and Hayashi, J. 2005. Nuclear DNA but not mtDNA controls tumor phenotypes in mouse cells. *Biochem. Biophys. Res. Commun.* 327: 1028–1035. [Medline] [CrossRef]
2. Augenlicht, L.H. and Heerdt, B.G. 2001. Mitochondria: integrators in tumorigenesis? *Nat. Genet.* 28: 104–105. [Medline] [CrossRef]
3. Balmain, A. and Nagase, H. 1998. Cancer resistance genes in mice: models for the study of tumour modifiers. *Trends Genet.* 14: 139–144. [Medline] [CrossRef]
4. Baysal, B.E., Ferrell, R.E., Willett-Brozick, J.E., Lawrence, E.C., Myssiorek, D., Bosch, A., van der Mey, A., Taschner, P.E., Rubinstein, W.S., Myers, E.N., Richard, C.W. 3rd., Cornelisse, C.J., Devilee, P., and Devlin, B. 2000. Mutations in SDHD, a mitochondrial complex II gene, in hereditary paraganglioma. *Science* 287: 848–851. [Medline] [CrossRef]
5. De Flora, S., D'Agostini, F., Masiello, L., Giunciuglio, D., and Albini, A. 1996. Synergism between N-acetylcysteine and doxorubicin in the prevention of tumorigenicity and metastasis in murine models. *Int. J. Cancer* 67: 842–848. [Medline] [CrossRef]
6. Fliss, M.S., Usadel, H., Caballero, O.L., Wu, L., Buta, M.R., Eleff, S.M., Jen, J., and Sidransky, D. 2000. Facile detection of mitochondrial DNA mutations in tumors and bodily fluids. *Science* 287: 2017–2019. [Medline] [CrossRef]
7. Gottlieb, E. and Tomlinson, I.P. 2005. Mitochondrial tumour suppressors: a genetic and biochemical update. *Nat. Rev. Cancer* 5: 857–866. [Medline] [CrossRef]
8. Harvey, M., McArthur, M.J., Montgomery, C.A. Jr., Bradley, A., and Donehower, L.A. 1993. Genetic background alters the spectrum of tumors that develop in p53-deficient mice. *FASEB J.* 7: 938–943. [Medline]
9. Hashizume, O., Shimizu, A., Yokota, M., Sugiyama, A., Nakada, K., Miyoshi, H., Itami, M., Ohira, M., Nagase, H., Takenaga, K., and Hayashi, J. 2012. Specific mitochondrial DNA mutation in mice regulates diabetes and lymphoma development. *Proc. Natl. Acad. Sci. USA* 109: 10528–10533. [Medline] [CrossRef]
10. He, Y., Wu, J., Dressman, D.C., Iacobuzio-Donahue, C., Markowitz, S.D., Velculescu, V.E., Diaz, L.A. Jr., Kinzler, K.W., Vogelstein, B., and Papadopoulos, N. 2010. Heteroplasmic mitochondrial DNA mutations in normal and tumour cells. *Nature* 464: 610–614. [Medline] [CrossRef]
11. Ishikawa, K., Takenaga, K., Akimoto, M., Koshikawa, N., Yamaguchi, A., Imanishi, H., Nakada, K., Honma, Y., and Hayashi, J. 2008. ROS-generating mitochondrial DNA mutations can regulate tumor cell metastasis. *Science* 320: 661–664. [Medline] [CrossRef]
12. Ishikawa, K., Hashizume, O., Koshikawa, N., Fukuda, S.,

Nakada, K., Takenaga, K., and Hayashi, J. 2008. Enhanced glycolysis induced by mtDNA mutations does not regulate metastasis. *FEBS Lett.* 582: 3525–3530. [Medline] [CrossRef]
13. Jacobs, H.T. 2003. The mitochondrial theory of aging: dead or alive? *Aging Cell* 2: 11–17. [Medline] [CrossRef]
14. Khrapko, K. and Vijg, J. 2009. Mitochondrial DNA mutations and aging: devils in the details? *Trends Genet.* 25: 91–98. [Medline] [CrossRef]
15. Klaunig, J.E., Kamendulis, L.M., and Hocevar, B.A. 2010. Oxidative stress and oxidative damage in carcinogenesis. *Toxicol. Pathol.* 38: 96–109. [Medline] [CrossRef]
16. Koppenol, W.H., Bounds, P.L., and Dang, C.V. 2011. Otto Warburg's contributions to current concepts of cancer metabolism. *Nat. Rev. Cancer* 11: 325–337. [Medline] [CrossRef]
17. Krupke, D.M., Begley, D.A., Sundberg, J.P., Bult, C.J., and Eppig, J.T. 2008. The Mouse Tumor Biology database. *Nat. Rev. Cancer* 8: 459–465. [Medline] [CrossRef]
18. Loeb, L.A., Wallace, D.C., and Martin, G.M. 2005. The mitochondrial theory of aging and its relationship to reactive oxygen species damage and somatic mtDNA mutations. *Proc. Natl. Acad. Sci. USA* 102: 18769–18770. [Medline] [CrossRef]
19. Niemann, S. and Müller, U. 2000. Mutations in SDHC cause autosomal dominant paraganglioma, type 3. *Nat. Genet.* 26: 268–270. [Medline] [CrossRef]
20. Pérez, V.I., Bokov, A., Van Remmen, H., Mele, J., Ran, Q., Ikeno, Y., and Richardson, A. 2009. Is the oxidative stress theory of aging dead? *Biochim. Biophys. Acta* 1790: 1005–1014. [Medline] [CrossRef]
21. Polyak, K., Li, Y., Zhu, H., Lengauer, C., Willson, J.K., Markowitz, S.D., Trush, M.A., Kinzler, K.W., and Vogelstein, B. 1998. Somatic mutations of the mitochondrial genome in human colorectal tumours. *Nat. Genet.* 20: 291–293. [Medline] [CrossRef]
22. Smyth, M.J., Hayakawa, Y., Takeda, K., and Yagita, H. 2002. New aspects of natural-killer-cell surveillance and therapy of cancer. *Nat. Rev. Cancer* 2: 850–861. [Medline] [CrossRef]
23. Taylor, R.W. and Turnbull, D.M. 2005. Mitochondrial DNA mutations in human disease. *Nat. Rev. Genet.* 6: 389–402. [Medline] [CrossRef]
24. Wallace, D.C. 1999. Mitochondrial diseases in man and mouse. *Science* 283: 1482–1488. [Medline] [CrossRef]
25. Yang, W. and Hekimi, S. 2010. A mitochondrial superoxide signal triggers increased longevity in *Caenorhabditis elegans*. *PLoS Biol.* 8: e1000556. [Medline] [CrossRef]
26. Yokota, M., Shitara, H., Hashizume, O., Ishikawa, K., Nakada, K., Ishii, R., Taya, C., Takenaga, K., Yonekawa, H., and Hayashi, J. 2010. Generation of trans-mitochondrial mitomice by the introduction of a pathogenic G13997A mtDNA from highly metastatic lung carcinoma cells. *FEBS Lett.* 584: 3943–3948. [Medline] [CrossRef]

1521-0103/352/2/338–345$25.00
THE JOURNAL OF PHARMACOLOGY AND EXPERIMENTAL THERAPEUTICS

http://dx.doi.org/10.1124/jpet.114.220673
J Pharmacol Exp Ther 352:338–345, February 2015

The Journal of PHARMACOLOGY And Experimental Therapeutics

# A Novel MitoNEET Ligand, TT01001, Improves Diabetes and Ameliorates Mitochondrial Function in db/db Mice[S]

Takehiro Takahashi, Masashi Yamamoto, Kazutoshi Amikura, Kozue Kato, Takashi Serizawa, Kanako Serizawa, Daisuke Akazawa, Takumi Aoki, Koji Kawai, Emi Ogasawara, Jun-Ichi Hayashi, Kazuto Nakada, and Mie Kainoh

*Toray Industries, Inc., Pharmaceutical Research Laboratories, Kanagawa, Japan (T.T., M.Y., K.A., Koz.K., T.S., K.S., D.A., T.A., Koj.K., M.K.); and Faculty of Life and Environmental Science, University of Tsukuba, Tsukuba, Ibaraki, Japan (E.O., J.-I.H., K.N.)*

Received November 18, 2014; accepted December 9, 2014

**ABSTRACT**

The mitochondrial outer membrane protein mitoNEET is a binding protein of the insulin sensitizer pioglitazone (5-[[4-[2-(5-ethylpyridin-2-yl)ethoxy]phenyl]methyl]-1,3-thiazolidine-2,4-dione) and is considered a novel target for the treatment of type II diabetes. Several small-molecule compounds have been identified as mitoNEET ligands using structure-based design or virtual docking studies. However, there are no reports about their therapeutic potential in animal models. Recently, we synthesized a novel small molecule, TT01001 [ethyl-4-(3-(3,5-dichlorophenyl)thioureido)piperidine-1-carboxylate], designed on the basis of pioglitazone structure. In this study, we assessed the pharmacological properties of TT01001 in both in vitro and in vivo studies. We found that TT01001 bound to mitoNEET without peroxisome proliferator-activated receptor-γ activation effect. In type II diabetes model db/db mice, TT01001 improved hyperglycemia, hyperlipidemia, and glucose intolerance, and its efficacy was equivalent to that of pioglitazone, without the pioglitazone-associated weight gain. Mitochondrial complex II + III activity of the skeletal muscle was significantly increased in db/db mice. We found that TT01001 significantly suppressed the elevated activity of the complex II + III. These results suggest that TT01001 improved type II diabetes without causing weight gain and ameliorated mitochondrial function of db/db mice. This is the first study that demonstrates the effects of a mitoNEET ligand on glucose metabolism and mitochondrial function in an animal disease model. These findings support targeting mitoNEET as a potential therapeutic approach for the treatment of type II diabetes.

## Introduction

Thiazolidinedione (TZD) derivatives, such as pioglitazone (5-[[4-[2-(5-ethylpyridin-2-yl)ethoxy]phenyl]methyl]-1,3-thiazolidine-2,4-dione) and rosiglitazone, are potent insulin sensitizers for the treatment of type II diabetes (Ahmadian et al., 2013). These ligands decrease serum triglycerides, free fatty acids, and inflammatory adipocytokines, such as tumor necrosis factor-α and interleukin-6, and increase the insulin-sensitizing hormone adiponectin by activating peroxisome proliferator-activated receptor-γ (PPARγ) (Kadowaki et al., 2006; Quinn et al., 2008). These various effects of TZD derivatives via the activation of PPARγ lead to the improvement of insulin resistance and glycemic parameters. Meanwhile, clinical side effects, such as weight gain or edema, are frequently observed in patients with type II diabetes treated with TZD derivatives and are attributed to PPARγ activation (Tang and Maroo, 2007; Borsting et al., 2012). Therefore, the clinical use of TZD derivatives has been limited in patients with heart failure or a past history of heart failure or renal dysfunction (Nissen and Wolski, 2007).

Mitochondria are known as the intracellular powerhouse of cells, and mitochondrial dysfunction is involved in a broad spectrum of diseases, both inherited and acquired (Andreux et al., 2013). In type II diabetes, many studies have focused on the association between the pathology of diabetes and mitochondrial dysfunction. Lower oxidative phosphorylation capacity was observed in muscle biopsy samples of patients with type II diabetes compared with those of healthy individuals (Kelley et al., 2002; Phielix et al., 2008; Ritov et al., 2010). The frequent reduction of mitochondrial contents was also shown in patients with type II diabetes (Hwang et al., 2010; Chomentowski et al., 2011). These reports indicate that mitochondrial function plays a key role in the pathology of type II diabetes. Recently, several reports have suggested that the TZD derivative pioglitazone directly influences mitochondrial function. For example, pioglitazone inhibits rat mitochondrial complex I activity in the liver and skeletal muscle tissue, indicating that alterations of cellular energy state by pioglitazone may contribute to the improvement in insulin sensitivity (Brunmair et al., 2004). Pioglitazone also increases the levels of the mitochondrial biogenesis regulator protein peroxisome proliferator-activated receptor-γ coactivator-1α (PGC-1α) in the skeletal muscle of db/db mice (Pagel-Langenickel et al., 2008). In patients with type II diabetes, pioglitazone treatment increases both mitochondrial

dx.doi.org/10.1124/jpet.114.220673.
[S] This article has supplemental material available at jpet.aspetjournals.org.

**ABBREVIATIONS:** DMSO, dimethyl sulfoxide; mtDNA, mitochondrial DNA; OGTT, oral glucose tolerance test; PCR, polymerase chain reaction; PPARγ, peroxisome proliferator-activated receptor-γ; RU, resonance unit; SPR, surface plasmon resonance; TR-FRET, time-resolved fluorescence resonance energy transfer; TT01001, ethyl-4-(3-(3,5-dichlorophenyl)thioureido)piperidine-1-carboxylate; TZD, thiazolidinedione.

DNA (mtDNA) copy numbers and the expression of PGC-1$\alpha$ in subcutaneous adipose tissue (Bogacka et al., 2005). These effects of pioglitazone are speculated to be independent of PPAR$\gamma$ activation (Feinstein et al., 2005). The mitochondrial outer membrane protein mitoNEET was identified as a novel binding protein of pioglitazone and has been considered a new target for type II diabetes therapies (Colca et al., 2004). Although the physiologic role of mitoNEET remains unclear, it is likely to modulate glucose metabolism or mitochondrial function. The mitochondria isolated from the heart of mitoNEET-deficient mice showed a decrease in state 3 respirations (Wiley et al., 2007). Overexpression of mitoNEET inside the adipose cell in genetic type II diabetic model ob/ob mice improved glycemic parameters and altered mitochondrial functions (Kusminski et al., 2012). Suppressed expression of mitoNEET in vitro decreased mitochondrial abilities (Sohn et al., 2013). Interestingly, the ligand for mitoNEET, NL-1, suppresses rotenone-induced toxicity in neuronal cells and mildly uncouples mitochondria (Geldenhuys et al., 2010). Other ligands for mitoNEET have also been reported by use of virtual docking studies (Bieganski and Yarmush, 2011). However, the in vivo effects of glucose metabolism or mitochondrial function have not been clarified for these mitoNEET ligands. Recently, we newly synthesized TT01001 [ethyl-4-(3-(3,5-dichlorophenyl)thioureido)piperidine-1-carboxylate], an orally active, small molecule that is designed on the basis of the pioglitazone structure. In this study, we first assessed the in vitro pharmacological profile of TT01001 with PPAR$\gamma$ activity and mitoNEET binding. Next, we examined the in vivo effects of TT01001 on diabetes and mitochondrial function using the type II diabetes murine model, db/db mice.

## Materials and Methods

**Chemicals.** The TT01001 (Fig. 1) was synthesized by the Pharmaceutical Laboratories, Toray Industries, Inc. (Kanagawa, Japan). Pioglitazone was purchased from Kemprotec Limited (Middlesbrough, Cambria, UK). All compounds were dissolved in dimethyl sulfoxide (DMSO) (Sigma-Aldrich, St. Louis, MO) for in vitro studies, or suspended in 0.5% (w/v) methyl cellulose (Nacarai Tesque, Kyoto, Japan) for in vivo studies.

**Protein Expression and Purification.** The protein expression and purification of the soluble human mitoNEET was performed as described previously with slight modification (Zuris et al., 2011). The gene of human mitoNEET (human kidney cDNA; Clontech, Mountain View, CA) was amplified by polymerase chain reaction (PCR) and cloned to the pCI-neo vector (Promega, Osaka, Japan). The fragment of mitoNEET encoding residues 33–108 was inserted into the pET-28b (+) vector (Novagen, Madison, WI) via the NdeI and XhoI sites, and the expression vector was introduced into *Escherichia coli* BL21 (DE3) cells. The mitoNEET protein was induced by the histidine-tagged protein by adding isopropyl-1-thio-$\beta$-D-galactoside (final concentration, 0.5 mmol/l) and culturing for 4 hours at 37°C. The *E. coli* pellets were collected and lysed by sonication in buffer A [50 mM Tris-hydrochloride (HCl) (pH 8.0), 250 mM NaCl, 5 mM imidazole] with 1 mM phenylmethylsulfonyl fluoride. The clarified supernatant was loaded onto a HisTrap HP (GE Healthcare, Tokyo, Japan) column pre-equilibrated with buffer A. The column was washed with buffer A, containing 100 mM imidazole, and the histidine-tagged mitoNEET protein was eluted with buffer A, containing 500 mM imidazole. To remove the histidine tag, the protein solution was incubated with restriction-grade thrombin (Novagen) for 6 hours at room temperature. The solution was loaded onto a HiTrap-Benzamidine tandem column (HisTrap HP and HiTrap Benzamidine FF; GE Healthcare), and the column was washed with the buffer containing 50 mM Tris-HCl (pH 8.0), 50 mM NaCl, and 100 mM imidazole. The flow-through and washing fractions were collected, and the protein was purified by size exclusion chromatography (HiLoad 16/60 Superdex 200 prep grade; GE Healthcare) in 50 mM Tris-HCl (pH 8.0), 50 mM NaCl.

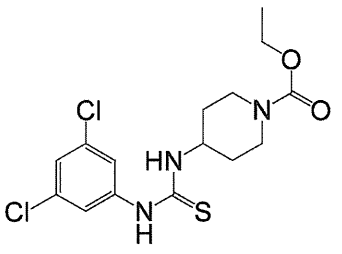


**Fig. 1.** Chemical structure of TT01001.

**Time-Resolved Fluorescence Resonance Energy Transfer Assay.** The PPAR$\gamma$ activation effect was assessed by the time-resolved fluorescence resonance energy transfer (TR-FRET) method using the LanthaScreen TR-FRET PPAR$\gamma$ coactivator assay kit (Invitrogen, Carlsbad, CA). The test compounds or solvent vehicle (DMSO) were incubated together with the human PPAR$\gamma$ ligand-binding domain tagged with glutathione *S*-transferase, terbium-labeled anti–glutathione *S*-transferase antibody, and fluorescein peptide with assay buffer. When binding of the test compound caused a conformational change in the PPAR$\gamma$ ligand-binding domain, excitation of terbium at 340 nm resulted in energy transfer and excitation of the fluorescein peptide, followed by emission at 520 nm. The signal at 520 nm was normalized by the signal obtained at 495 nm. Each assay was performed in quadruplicate and the data were expressed as the mean ratios of 520 and 495 nm. The mean ratios were plotted against the concentration of the test compounds.

**Surface Plasmon Resonance Interaction Analysis.** The surface plasmon resonance (SPR) measurements were carried out by the Biacore S51 instrument (Biacore AB, Uppsala, Sweden). The mitoNEET protein was immobilized onto the sensor chip (CM-5; GE Healthcare) using the amine coupling method. Different concentrations of TT01001 (1, 2, 4, 8, and 20 $\mu$mol/l) and pioglitazone (0.3, 0.6, 1.3, 2.5, and 5.0 $\mu$mol/l) were injected for 60 seconds at a flow rate of 30 $\mu$l/min. The resonance unit (RU) curves were normalized by the reference surface and no-response concentration using S51 evaluation software (GE Healthcare).

**Animals and Administration of Compounds.** This study was reviewed by the Animal Care and Use Committee, approved by the head of the test facility, and performed in accordance with the Guidelines for Animal Experiments, Research and Development Division, Toray Industries, Inc. Male, 5-week-old mice of C57BL/6J and BKS.Cg-+ *Lepr$^{db}$*/+*Lepr$^{db}$* (db/db) were obtained from CLEA Japan, Inc. (Tokyo, Japan). All mice were group-housed in cages at 22–24°C with a 12-hour light/dark cycle (lights on at 7:00 AM) for 1 week before the experiments began. Mice were given ad libitum access to food and water. In db/db mice, the vehicle (0.5% methyl cellulose) or test compounds were orally administered once daily for 28 days. The vehicle was also given to C57BL/6J mice orally once daily for 28 days.

**Analysis of Blood Glucose, Glucose Intolerance, and Plasma Parameters.** We obtained whole blood samples (approximately 5 $\mu$l) from the tail vein under postprandial conditions and measured blood glucose with an automatic glucometer (Precision Exceed; Abbott Diabetes Care Ltd., Alameda, CA) on day 27 before final dosing. On day 28, we determined fasting blood glucose levels and performed oral glucose tolerance tests (OGTTs) under 18-hour fasting conditions. Blood glucose concentrations were quantified before and after glucose loading (1.5 g/kg p.o.) at different time points (0, 30, 60, 90, 120, 150, and 180 minutes) by the aforementioned method. On day 28, for plasma sampling, we also placed the mice under isoflurane anesthesia and collected whole blood from the inferior vena cava under postprandial conditions. Plasma samples were obtained by centrifugation at 3000 rpm at 4°C for 10 minutes. Plasma insulin and nonesterified fatty acid levels were determined by enzyme-linked immunosorbent assay (Shibayagi, Gunnma,

Japan) and the colorimetric method (Wako Pure Chemical Industries, Osaka, Japan).

**mtDNA Determination by Quantitative Real-Time PCR.** We sacrificed vehicle or test compound-treated mice on day 28 by bleeding under anesthesia, rapidly removed the skeletal muscle (soleus and gastrocnemius muscle), and immediately froze it with liquid nitrogen. We isolated total DNA from the skeletal muscle using the QIAamp DNA Mini Kit (QIAGEN, Valencia, CA). The mtDNA level was quantified using the TaqMan gene expression assay system (Applied Biosystems, Foster City, CA). The PCR reaction was carried out in a 20 $\mu$l volume containing 2× TaqMan Universal Master Mix (Applied Biosystems), PCR-grade water (Roche Diagnostic Japan, Tokyo, Japab), TaqMan probes for the D-loop and thymidine kinase 1 regions, and the total DNA sample. The TaqMan probe sequence is shown in Supplemental Table 1. We conducted PCR amplification with 40 cycles of the program at 95°C for 20 seconds, 95°C for 3 seconds, and 60°C for 30 seconds. Each sample was assayed in duplicate and the fluorescence spectra were continuously monitored by the 7500 Fast Real-Time PCR system with Sequence Detection Software, version 1.4 (Applied Biosystems/Life Technologies, Carlsbad, CA). Data analysis was based on measurement of the cycle threshold ($C_t$). The mtDNA copy number was determined from the standard curve and normalized by division of the D-loop value by the thymidine kinase 1 value. The data were expressed as relative values against the mtDNA level in C57BL/6J mice and shown as mean ± S.E.M.

**Isolation of the Mitochondrial Fraction.** We obtained skeletal muscle from the sacrificed mice and homogenized it with homogenizing buffer (0.2 M sucrose, 0.13 M NaCl, 1.0 mM Tris-HCl, pH = 7.4) on ice. The homogenized sample was centrifuged at 3000 rpm for 10 minutes at 4°C and the supernatant was again centrifuged at 14,000 rpm for 10 minutes. The supernatant was removed and the pellet (i.e., the mitochondrial fraction) was dissolved in 0.25 M sucrose. The mitochondrial fraction was frozen and thawed twice to assess mitochondrial respiratory chain enzyme activity.

**Measurement of Mitochondrial Respiratory Chain Enzyme Activity.** To evaluate the short-duration effect of the test compounds on mitochondrial function, we assessed respiratory chain enzyme activity of the skeletal muscle mitochondrial fraction in db/db mice. Moreover, the mitochondrial function of compound-treated db/db mice was used to evaluate the chronic effect of test compounds on mitochondrial function. The assay was conducted as described previously, with slight modifications (Spinazzi et al., 2012). The reaction was carried out in 200 $\mu$l volume and detected by a microplate reader (SpectraMax 190; Molecular Devices, Sunnyvale, CA). The test compounds or DMSO were directly added to the reaction buffer (final concentration of DMSO was 1%) to assess the short-duration effects of the test compounds. Mitochondrial complex specific inhibitor, rotenone, malonate, and KCN were used as the reference compounds. Citrate synthase activity was measured as follows. The mitochondrial fraction was incubated in buffer containing 0.1 mM 5,5′-dithiobis(2-nitrobenzoic acid) and 0.3 mM acetyl-CoA at 37°C for 5 minutes. The reaction was started by adding 0.5 mM oxaloacetic acid, and then we monitored the increase in absorbance at 412 nm for 3 minutes. Complex I + III and II + III activities were measured by reduction of oxidized cytochrome *c* at an absorbance of 550 nm. In complex I + III activity, 50 mM Tris-HCl, 1 mM KCN, 0.1 mM NADH, and 0.1 mM oxidized cytochrome *c* were incubated at 37°C for 5 minutes. The reaction was started by adding the sample, and the absorbance was observed for 3 minutes. In complex II + III activity, 5 mM potassium phosphate buffer, 2 mM KCN, 10 mM sodium succinate dibasic, and the sample were incubated at 37°C for 10 minutes. The reaction was started by adding 0.1 mM oxidized cytochrome *c*, and the absorbance change was observed for 3 minutes. Complex IV activity was measured by oxidation of reduced cytochrome *c* in absorbance at 550 nm. Reduced cytochrome *c* was prepared as described previously (Spinazzi et al., 2012). We incubated 5 mM potassium phosphate buffer and reduced cytochrome *c* at 37°C for 5 minutes. The reaction was started by adding the sample, and the absorbance change was observed for 3 minutes. The results of complex I + III, II + III, and IV activities were normalized by citrate synthase activity. Because of the variability of citrate synthase activity in each sample, respiratory chain enzyme activities were also normalized to each protein concentration. Data were expressed as relative values against vehicle-treated C57BL/6J mice enzyme activities and shown as mean ± S.E.M.

**Data and Statistical Analyses.** All data were expressed as mean ± S.E.M. We calculated the areas under the curves using the trapezoidal rule from the blood glucose in the OGTT in C57BL/6J or db/db mice. We performed the statistical analysis using one-way analysis of variance followed by Dunnett's multiple comparison in three groups. A $P$ value of $< 0.05$ was considered statistically significant.

## Results

**TT01001 Did Not Activate PPARγ but Interacted with MitoNEET.** To evaluate the pharmacological properties of TT01001, we first examined the PPARγ activation effect by the TR-FRET method. No change in TR-FRET emission signal of TT01001 was seen in the concentration range of 0.001–100 $\mu$mol/l. On the other hand, pioglitazone increased the TR-FRET emission signals in a concentration-dependent manner (Fig. 2A). Next, to evaluate the binding effect of TT01001 for mitoNEET, we assessed the effect of TT01001 on mitoNEET protein by the SPR method using the Biacore instrument. The injection of TT01001 onto immobilized mitoNEET increased the RU in a concentration-dependent manner (1, 2, 4, 8, and 20 $\mu$mol/l) (Fig. 2B). Pioglitazone also increased the RU in a concentration-dependent manner (0.3, 0.6, 1.2, 2.5, and 5.0 $\mu$mol/l) (Fig. 2C).

**TT01001 Improved Diabetes in db/db Mice without Causing Weight Gain.** We next evaluated whether TT01001 could exhibit an ameliorative effect on glycemic parameters in vivo. We orally administered either TT01001 (100 mg/kg) or pioglitazone (30 mg/kg) to a genetically obese rodent model, db/db mice, once daily for 28 days. There was no effect of TT01001 on body weight, but it was increased by pioglitazone in a duration-dependent manner (Fig. 3A). On day 24, there were no body weight changes in TT01001-treated db/db mice; meanwhile, there was a significant increase in body weight in pioglitazone-treated db/db mice compared with vehicle-treated db/db mice (Fig. 3B). As for glycemic parameters, TT01001 treatment significantly decreased blood glucose levels (postprandial and fasting) (Fig. 3, C and D). During the OGTT, blood glucose levels were lower in TT01001-treated db/db mice than in vehicle-treated db/db mice at all measurement points (Fig. 3E). Glucose areas under the curve (0–180 minutes in OGTT) were significantly decreased in TT01001-treated db/db mice (Fig. 3F). In the plasma parameters of vehicle-treated db/db mice, a significant decrease was seen in the relative value of the endpoint of insulin concentration against the beginning of dosage compared with C57BL/6J mice. Neither TT01001 nor pioglitazone affected the plasma insulin levels (Fig. 3G). With regard to dyslipidemia, vehicle-treated db/db mice exhibited hyperlipidemia compared with C57BL/6J mice. There were significantly lower plasma nonesterified fatty acid levels in TT01001-treated db/db mice, similar to the changes seen with pioglitazone (Fig. 3H).

**Effect of TT01001 on mtDNA Levels and Mitochondrial Respiratory Chain Enzyme Activity.** To reveal the effect of TT01001 on mitochondrial function, we examined the effects on mtDNA levels and mitochondrial respiratory chain enzyme activity in the skeletal muscle. The mtDNA level was significantly decreased in vehicle-treated db/db mice compared with that in C57BL/6J mice. Meanwhile, there were no differences

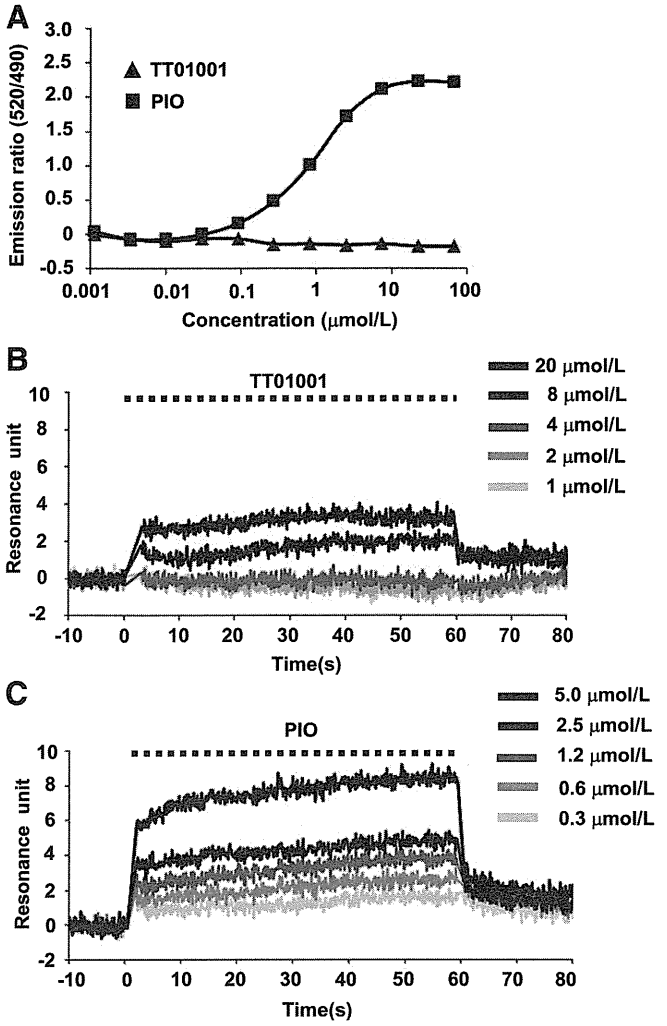


**Fig. 2.** TT01001 did not activate PPARγ but interacted with mitoNEET. The activity of PPARγ was assessed by the TR-FRET method using the LanthaScreen TR-FRET PPARγ coactivator assay kit (Invitrogen). TT01001 or pioglitazone (PIO) was incubated with the human PPARγ ligand-binding domain tagged with glutathione *S*-transferase, terbium-labeled anti–glutathione *S*-transferase antibody, and fluorescein peptide. Each line is expressed as a mean emission ratio of 520 and 495 nm ($N = 4$). (A) The interaction of TT01001 and PIO was determined by the SPR method using Biacore S51 (Biacore AB). Different concentrations of TT01001 or PIO were injected onto the immobilized mitoNEET on a sensor chip (CM-5; GE Healthcare) for 60 seconds at a flow rate of 30 μl/min. Each line indicates the RU curves of (B) 1, 2, 4, 8, and 20 μmol/l TT01001 and (C) 0.3, 0.6, 1.2, 2.5, and 5.0 μmol/, PIO, respectively.

in the mtDNA level of TT01001- or pioglitazone-treated db/db mice (Fig. 4). In addition to analyzing the mtDNA levels, we examined mitochondrial chain enzyme activity, and complex I + III, II + III, and IV activity in db/db mice. First, we examined the short-duration effect of the test compounds on the mitochondrial respiratory chain enzyme activity of the skeletal muscle in db/db mice. There were no alterations in complex I + II, II + III, and IV activities with either TT01001 or pioglitazone (10 or 30 μmol/l, respectively) (Fig. 5, A–C). We next examined the chronic effects of the test compounds on mitochondrial respiratory chain enzyme activity in the skeletal muscle of db/db mice. There was no change in complex I + III or IV activity of vehicle- or test compound–treated db/db mice compared with C57BL/6J mice (Fig. 6, A and C). Meanwhile, complex II + III activity was approximately 2-fold higher in vehicle-treated db/db mice than in C57BL/6J mice (Fig. 6B). We found that TT01001 significantly decreased elevated complex II + III activity compared with that in vehicle-treated mice.

## Discussion

The mitochondrial outer membrane protein mitoNEET, a binding protein of the insulin sensitizer pioglitazone, is considered a novel drug target for the treatment of type II diabetes (Colca et al., 2004). Kushiminski et al. (2012) demonstrated that the overexpression of mitoNEET in adipose tissues improved glycemic parameters, altered mitochondrial function, and decreased β-oxidation or membrane potentials. That report suggested an in vivo physiologic role of mitoNEET in glucose metabolism or mitochondrial function. On the other hand, although targeting mitoNEET is considered a novel strategy for the treatment of type II diabetes; there were no reports on the mitoNEET ligand effect on diabetes or mitochondrial function using animal disease models. In this study, we demonstrated the first experimental observation of the effects of the mitoNEET ligand on diabetes and mitochondrial function in type II diabetic model db/db mice.

Recently, we synthesized a new small-molecule compound called TT01001 on the basis of the pioglitazone structure. Pioglitazone has been known as a PPARγ agonist (Lehmann et al., 1995), thus we first examined the PPARγ activation effect of TT01001. TT01001 did not change TR-FRET emission signal; meanwhile, pioglitazone showed the increase of TR-FRET emission signal in a concentration-dependent manner. These results suggest that TT01001 did not show the activation effect of PPARγ. We next assessed the binding effect of TT01001 to mitoNEET by using recombinant mitoNEET and the SPR method. TT01001 increased the RU in a concentration-dependent manner, similar to pioglitazone on the immobilized recombinant mitoNEET. Previously, the binding effect of pioglitazone to mitoNEET was observed using liver mitochondrial suspension (Geldenhuys et al., 2010). Therefore, our SPR data suggest that TT01001 has a binding effect on mitoNEET. Collectively, TT01001 has in vitro pharmacological characteristics similar to the mitoNEET binding effect, but not a PPARγ activation effect.

To clarify whether oral administration of TT01001 could exhibit an ameliorative effect on diabetes, we examined the effects of TT01001 on glycemic parameters in db/db mice. Oral administration of TT01001 for 28 days significantly reduced blood glucose levels (postprandial and fasting) and improved glucose intolerance and hyperlipidemia, but not plasma insulin levels. These effects of TT01001 were almost equivalent to those of pioglitazone, indicating that TT01001 has a potent antidiabetic effect. Pioglitazone improves hyperglycemia and hyperlipidemia of db/db mice via an insulin-sensitizing effect on peripheral tissues (Suzuki et al., 2000). Thus, our data suggest that TT01001 improved peripheral glucose and lipid utilization in a manner similar to pioglitazone. In contrast to the apparent effects on glucose metabolism, pioglitazone significantly increased body weight in db/db mice. Weight gain is one of the major side effects of pioglitazone in clinical use (Gillies and Dunn, 2000), and it is attributed to pioglitazone's enhancement of PPARγ activation (Borsting et al., 2012). Therefore, weight gain in pioglitazone-treated db/db mice is considered a hallmark side effect of pioglitazone in clinical use. Interestingly, TT01001 has equivalent efficacy with pioglitazone on

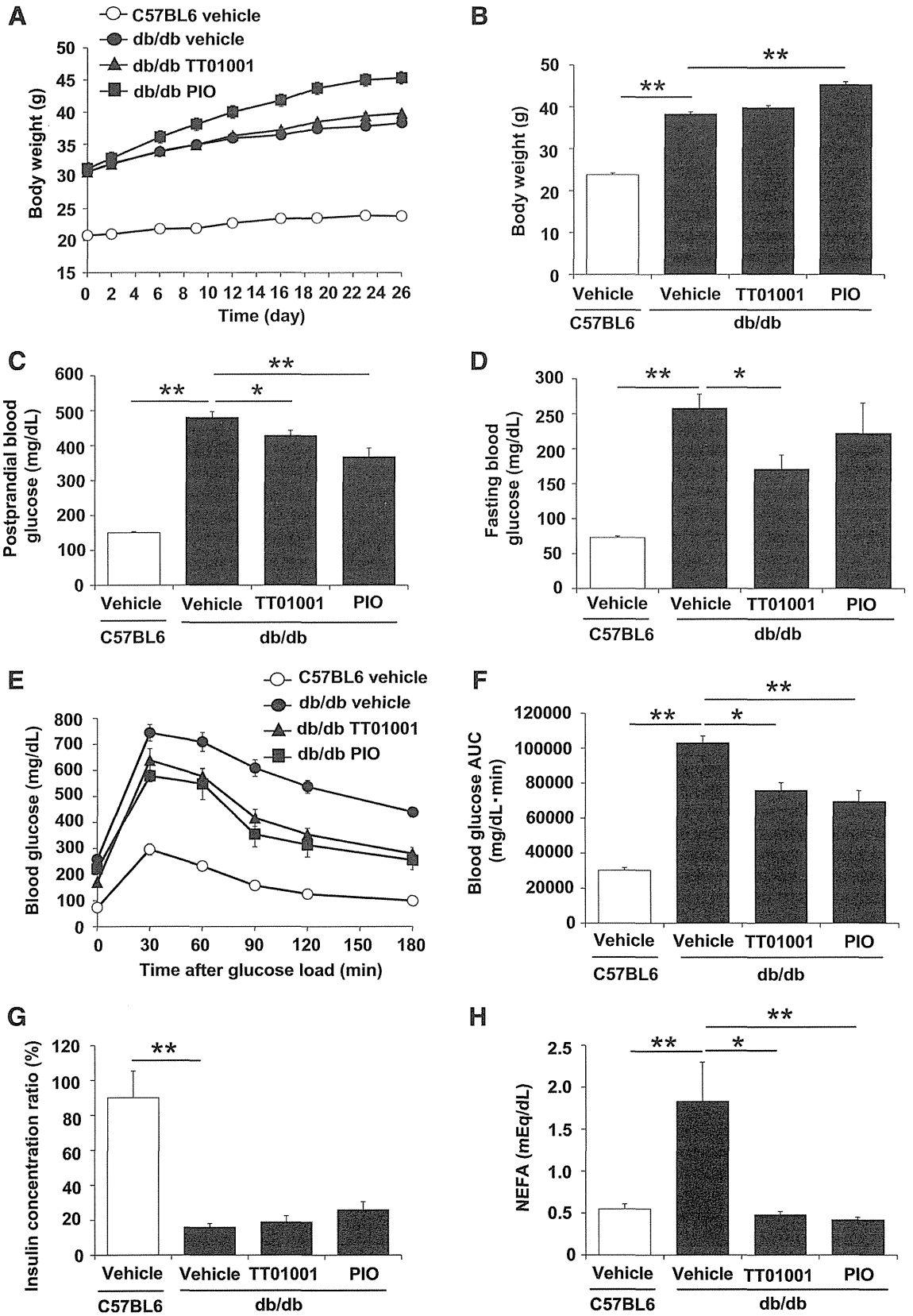


**Fig. 3.** TT01001 improved diabetes in db/db mice without causing weight gain. The vehicle (0.5% methyl cellulose), TT01001 (100 mg/kg), or pioglitazone (PIO; 30 mg/kg) were orally administered to db/db mice once daily for 28 days. The vehicle was also orally administered to C57BL/6J mice. The courses of (A) body weight ($N = 14$), (B) body weight on day 24 ($N = 14$), (C) postprandial blood glucose levels ($N = 14$), (D) fasting blood glucose levels ($N = 8$), (E) blood glucose levels during the OGTT ($N = 8$), (F) blood glucose areas under the curves (0–180 minutes) ($N = 8$), (G) ratio of plasma insulin concentration between the beginning of dosage and end of dosage ($N = 6$), and (H) plasma concentration of nonesterified fatty acid ($N = 6$) are shown as means ± S.E.M. $^*P < 0.05$; $^{**}P < 0.01$ compared with the vehicle-treated db/db mice by Dunnett's multiple test.

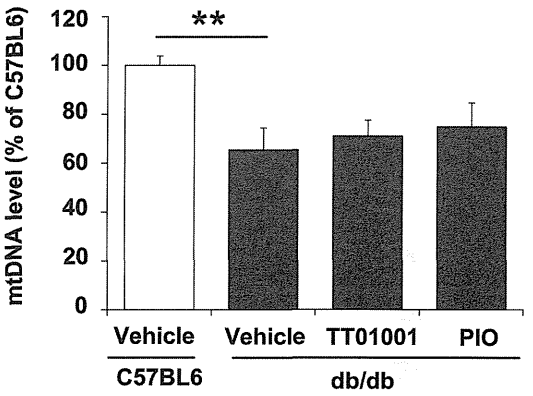


**Fig. 4.** TT01001 and pioglitazone (PIO) did not affect the mtDNA level in the skeletal muscle of db/db mice. The vehicle (0.5% methyl cellulose), TT01001 (100 mg/kg), or PIO (30 mg/kg) was orally administered to db/db mice once daily for 28 days. The vehicle was also orally administered to C57BL/6J mice. The mtDNA levels were determined by quantitative real-time PCR. Data are shown as means of the mtDNA ratio against C57BL/6J mice ± S.E.M. $^{**}P < 0.01$ compared with the vehicle-treated db/db mice by Dunnett's multiple test ($N = 6$ animals per group).

glycemic parameters, whereas it has no effect on body weight in db/db mice. As the possible reason for this phenomenon, although TT01001 bound to mitoNEET in a manner similar to pioglitazone, it did not exhibit the PPAR$\gamma$ activation effect. Taken together, TT01001 has therapeutic efficacy equivalent to the insulin-sensitizer pioglitazone without causing weight gain in db/db mice.

Isolated heart mitochondria of mitoNEET-deficient mice show a decrease in state 3 respirations (Wiley et al., 2007). The overexpression of mitoNEET in genetic type II diabetic model ob/ob mice showed the alteration of mitochondrial functions (Kusminski et al., 2012). These reports may indicate that mitoNEET plays a physiologic role in mitochondrial function. To examine the effects of TT01001 on mitochondrial function, we first examined the effect of TT01001 on mitochondrial biogenesis in the skeletal muscle, which is a major target organ of insulin and plays an essential role in glucose utilization (DeFronzo et al., 1979) in db/db mice. We observed significantly lower levels of mtDNA in vehicle-treated db/db mice compared with C57BL/6J mice. Since the mtDNA level is closely related to the pathology of type II diabetes (Lee et al., 1998; Song et al., 2001), decreased mtDNA levels in the skeletal muscle of vehicle-treated db/db mice were considered an alteration of mitochondrial function. However, we did not find that TT01001 and pioglitazone affected the mtDNA level in the skeletal muscle of db/db mice. A previous study showed that pioglitazone increased mtDNA copy numbers in the subcutaneous adipose tissue of patients with type II diabetes for 12 weeks after administration (Bogacka et al., 2005). Although the effects of TT01001 and pioglitazone on the mtDNA levels in adipose tissue are unknown, they may have no effect on the amount of mtDNA in skeletal muscle during an administration period of this length. Collectively, these data suggest that TT01001, at least in the skeletal muscle, did not have an effect on mitochondrial biogenesis.

In the mitochondrial respiratory chain enzyme activity assay, TT01001 did not affect complex I + III, II + III, or IV activity of the isolated mitochondrial fraction of the skeletal muscle from db/db mice during a short time period. On the other hand, in a chronic examination, TT01001 led to a significant

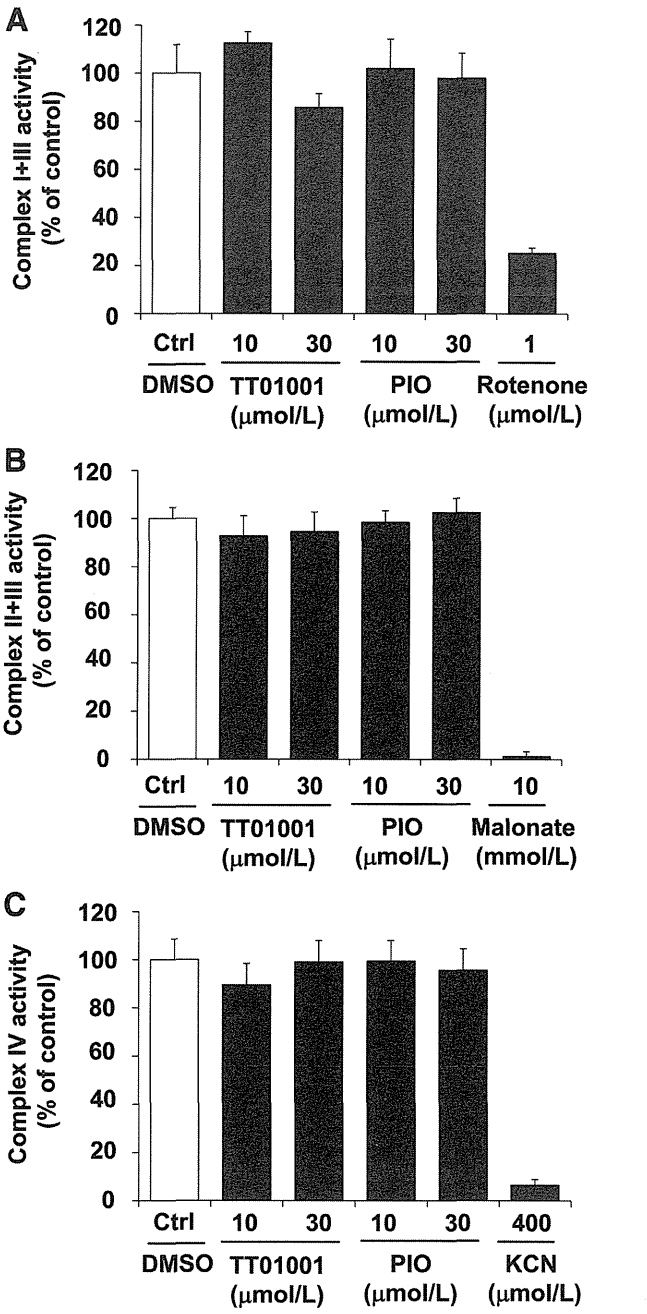


**Fig. 5.** TT01001 and pioglitazone (PIO) did not affect mitochondrial respiratory chain enzyme activity during a short time period. DMSO, TT01001, or PIO was applied to the skeletal muscle mitochondrial fraction of db/db mice, and mitochondrial respiratory chain enzyme activity was measured by complex (A) I + III, (B) complex II + III, and (C) complex IV activities. Complex activity was normalized by citrate synthase activity in each sample. Mitochondrial complex-specific inhibitor, rotenone, malonate, and KCN were used as the reference compounds. Each assay was performed in triplicate and the data are shown as the means of ratios against the control (DMSO treatment) ± S.E.M. Incubation times of TT01001 and PIO are 5 minutes for the complex I + III and complex IV activity assays and 10 minutes for the complex II + III activity assay, respectively.

reduction in the increase of complex II + III activity without having an effect on complex I + III or IV activity in the skeletal muscle of db/db mice. In db/db mice, mitochondrial respiration of the glycolytic skeletal muscle is enhanced under physiologic conditions (Holmström et al., 2012). Excess lipid increased the oxidative capacity and expression level of the mitochondrial

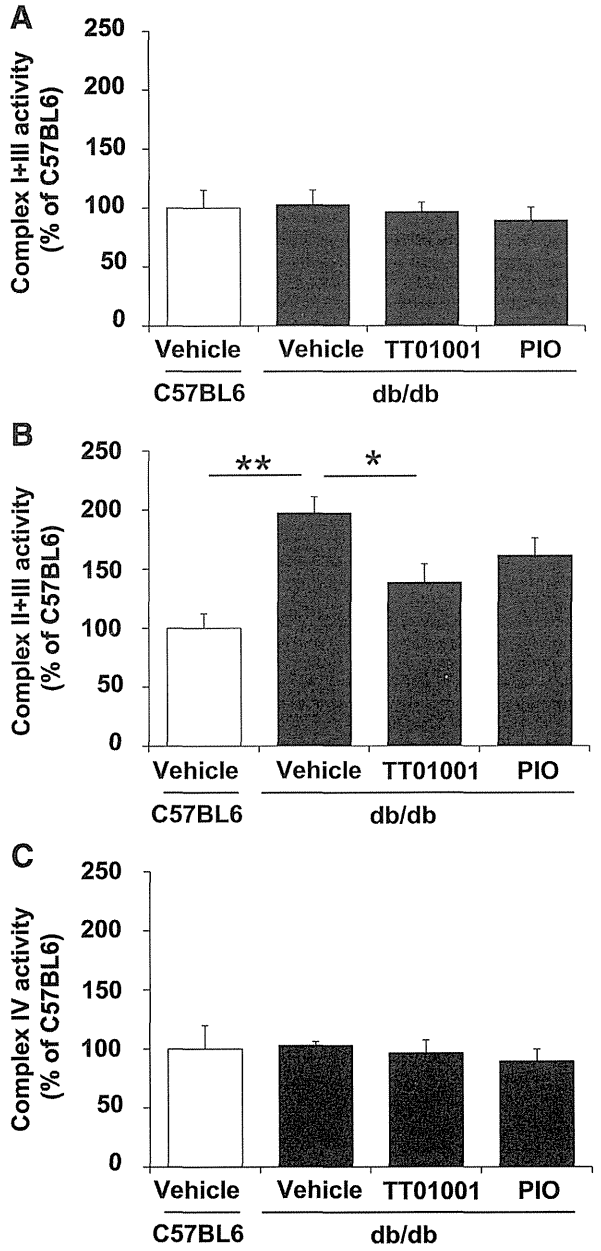


**Fig. 6.** TT01001 decreased elevated complex II + III activity in db/db mice. The vehicle (0.5% methyl cellulose), TT01001 (100 mg/kg), or pioglitazone (PIO; 30 mg/kg) was orally administered to db/db mice once daily for 28 days. The vehicle was also orally administered to C57BL/6J mice. The mitochondrial fraction was isolated from vehicle- or compound-treated mice, and mitochondrial respiratory chain enzyme activity was measured by (A) complex I + III, (B) complex II + III, and (C) complex IV activities. The data are shown as the means of ratios against vehicle-treated C57BL/6J mice ± S.E.M. $*P < 0.05$, $**P < 0.01$ compared with the vehicle-treated db/db mice by Dunnett's multiple test ($N = 6$ animals per group).

respiratory chain subunit in the skeletal muscle of db/db mice (Turner et al., 2007). Possibly, as a result of enhanced complex II + III activity in db/db mice this might indicate that it is a compensatory response to diabetic conditions, hyperglycemia, or hyperlipidemia. The skeletal muscle mitochondrial complex II has been reported to produce superoxide and/or hydrogen peroxide at relatively high rates (Quinlan et al., 2012). Accordingly, we speculate that compensatory enhanced complex II + III activity leads to high production of superoxide and/or hydrogen peroxide, and they, at least in part, contribute to type II diabetes conditions in db/db mice. It is possible that mitoNEET contributes to modulating oxidative stress via transferring iron into the mitochondrial matrix (Zuris et al., 2011). TT01001 might ameliorate mitochondrial function toward normalization through the modulation of oxidative stress in the skeletal muscle of db/db mice. Therefore, mitoNEET may be a key regulatory protein of mitochondrial function, especially respiratory chain enzyme complex II or oxidative stress modulation. On the other hand, it was not clear how TT01001 suppressed the increase in complex II + III activity with no effect on mitochondrial biogenesis or complex I + III and IV activity. The practical concentration of TT01001 in target tissues and the binding affinity of it to mitoNEET have been unknown. Thus, a detailed analysis of mitoNEET on type II diabetes or mitochondrial function and pharmacokinetics-pharmacodynamics profiles of TT01001 is needed to elucidate the mechanism of action of TT01001. Further examination might identify the physiologic role of mitoNEET in type II diabetes or mitochondrial function.

In conclusion, our results show that the orally active, small-molecule TT01001 showed binding affinity for mitoNEET without a PPARγ activation effect. It improved diabetes and ameliorated mitochondrial function in the skeletal muscle of db/db mice. This is the first study that demonstrates the effects of a mitoNEET ligand on glucose metabolism and mitochondrial function in a type II diabetic animal model. Although further study is needed to clarify the physiologic role of mitoNEET in diabetes and mitochondrial function, our data suggest that the alteration of mitochondrial function via mitoNEET may be valuable for the treatment of type II diabetes. Finally, this study would support targeting mitoNEET as a useful therapeutic approach for the treatment of type II diabetes.

#### Acknowledgments

The authors thank Hiroki Kumagai, Naoyoshi Yamamoto, and Yosuke Iura for fruitful discussions; and Yumiko Sekiya, Seiji Okazaki, Tomokatsu Iwamura, Junko Kanda, Hiroe Hirokawa, Hiroyuki Meguro, and Rie Sasaki for excellent technical assistance.

#### Authorship Contributions

*Participated in research design:* Takahashi, Yamamoto, Ogasawara, Hayashi, Nakada, Kainoh.

*Conducted experiments:* Takahashi, Amikura, Kato, T. Serizawa, K. Serizawa, Akazawa.

*Contributed new reagents or analytic tools:* Yamamoto, Aoki, Kawai.

*Performed data analysis:* Takahashi.

*Wrote or contributed to the writing of the manuscript:* Takahashi, Ogasawara, Nakada, Kainoh.

#### References

Ahmadian M, Suh JM, Hah N, Liddle C, Atkins AR, Downes M, and Evans RM (2013) PPARγ signaling and metabolism: the good, the bad and the future. *Nat Med* **19:** 557–566.

Andreux PA, Houtkooper RH, and Auwerx J (2013) Pharmacological approaches to restore mitochondrial function. *Nat Rev Drug Discov* **12:**465–483.

Bieganski RM and Yarmush ML (2011) Novel ligands that target the mitochondrial membrane protein mitoNEET. *J Mol Graph Model* **29:**965–973.

Bogacka I, Xie H, Bray GA, and Smith SR (2005) Pioglitazone induces mitochondrial biogenesis in human subcutaneous adipose tissue in vivo. *Diabetes* **54:**1392–1399.

Borsting E, Cheng VP, Glass CK, Vallon V, and Cunard R (2012) Peroxisome proliferator-activated receptor-γ agonists repress epithelial sodium channel expression in the kidney. *Am J Physiol Renal Physiol* **302:**F540–F551.

Brunmair B, Staniek K, Gras F, Scharf N, Althaym A, Clara R, Roden M, Gnaiger E, Nohl H, Waldhäusl W, et al. (2004) Thiazolidinediones, like metformin, inhibit respiratory complex I: a common mechanism contributing to their antidiabetic actions? *Diabetes* **53:**1052–1059.

Chomentowski P, Coen PM, Radiková Z, Goodpaster BH, and Toledo FG (2011) Skeletal muscle mitochondria in insulin resistance: differences in intermyofibrillar versus subsarcolemmal subpopulations and relationship to metabolic flexibility. *J Clin Endocrinol Metab* **96:**494–503.

Colca JR, McDonald WG, Waldon DJ, Leone JW, Lull JM, Bannow CA, Lund ET, and Mathews WR (2004) Identification of a novel mitochondrial protein ("mitoNEET") cross-linked specifically by a thiazolidinedione photoprobe. *Am J Physiol Endocrinol Metab* **286:**E252–E260.

DeFronzo RA, Tobin JD, and Andres R (1979) Glucose clamp technique: a method for quantifying insulin secretion and resistance. *Am J Physiol* **237:**E214–E223.

Feinstein DL, Spagnolo A, Akar C, Weinberg G, Murphy P, Gavrilyuk V, and Dello Russo C (2005) Receptor-independent actions of PPAR thiazolidinedione agonists: is mitochondrial function the key? *Biochem Pharmacol* **70:**177–188.

Geldenhuys WJ, Funk MO, Barnes KF, and Carroll RT (2010) Structure-based design of a thiazolidinedione which targets the mitochondrial protein mitoNEET. *Bioorg Med Chem Lett* **20:**819–823.

Gillies PS and Dunn CJ (2000) Pioglitazone. *Drugs* **60:**333–343; discussion 344–345.

Holmström MH, Iglesias-Gutierrez E, Zierath JR, and Garcia-Roves PM (2012) Tissue-specific control of mitochondrial respiration in obesity-related insulin resistance and diabetes. *Am J Physiol Endocrinol Metab* **302:**E731–E739.

Hwang H, Bowen BP, Lefort N, Flynn CR, De Filippis EA, Roberts C, Smoke CC, Meyer C, Højlund K, Yi Z, et al. (2010) Proteomics analysis of human skeletal muscle reveals novel abnormalities in obesity and type 2 diabetes. *Diabetes* **59:** 33–42.

Kadowaki T, Yamauchi T, Kubota N, Hara K, Ueki K, and Tobe K (2006) Adiponectin and adiponectin receptors in insulin resistance, diabetes, and the metabolic syndrome. *J Clin Invest* **116:**1784–1792.

Kelley DE, He J, Menshikova EV, and Ritov VB (2002) Dysfunction of mitochondria in human skeletal muscle in type 2 diabetes. *Diabetes* **51:**2944–2950.

Kusminski CM, Holland WL, Sun K, Park J, Spurgin SB, Lin Y, Askew GR, Simcox JA, McClain DA, Li C, et al. (2012) MitoNEET-driven alterations in adipocyte mitochondrial activity reveal a crucial adaptive process that preserves insulin sensitivity in obesity. *Nat Med* **18:**1539–1549.

Lee HK, Song JH, Shin CS, Park DJ, Park KS, Lee KU, and Koh CS (1998) Decreased mitochondrial DNA content in peripheral blood precedes the development of non-insulin-dependent diabetes mellitus. *Diabetes Res Clin Pract* **42:**161–167.

Lehmann JM, Moore LB, Smith-Oliver TA, Wilkison WO, Willson TM, and Kliewer SA (1995) An antidiabetic thiazolidinedione is a high affinity ligand for peroxisome proliferator-activated receptor gamma (PPAR gamma). *J Biol Chem* **270:**12953–12956.

Nissen SE and Wolski K (2007) Effect of rosiglitazone on the risk of myocardial infarction and death from cardiovascular causes. *N Engl J Med* **356:**2457–2471.

Pagel-Langenickel I, Bao J, Joseph JJ, Schwartz DR, Mantell BS, Xu X, Raghavachari N, and Sack MN (2008) PGC-1alpha integrates insulin signaling, mitochondrial regulation, and bioenergetic function in skeletal muscle. *J Biol Chem* **283:**22464–22472.

Phielix E, Schrauwen-Hinderling VB, Mensink M, Lenaers E, Meex R, Hoeks J, Kooi ME, Moonen-Kornips E, Sels JP, Hesselink MK, et al. (2008) Lower intrinsic ADP-stimulated mitochondrial respiration underlies in vivo mitochondrial dysfunction in muscle of male type 2 diabetic patients. *Diabetes* **57:**2943–2949.

Quinlan CL, Orr AL, Perevoshchikova IV, Treberg JR, Ackrell BA, and Brand MD (2012) Mitochondrial complex II can generate reactive oxygen species at high rates in both the forward and reverse reactions. *J Biol Chem* **287:**27255–27264.

Quinn CE, Hamilton PK, Lockhart CJ, and McVeigh GE (2008) Thiazolidinediones: effects on insulin resistance and the cardiovascular system. *Br J Pharmacol* **153:** 636–645.

Ritov VB, Menshikova EV, Azuma K, Wood R, Toledo FG, Goodpaster BH, Ruderman NB, and Kelley DE (2010) Deficiency of electron transport chain in human skeletal muscle mitochondria in type 2 diabetes mellitus and obesity. *Am J Physiol Endocrinol Metab* **298:**E49–E58.

Sohn YS, Tamir S, Song L, Michaeli D, Matouk I, Conlan AR, Harir Y, Holt SH, Shulaev V, Paddock ML, et al. (2013) NAF-1 and mitoNEET are central to human breast cancer proliferation by maintaining mitochondrial homeostasis and promoting tumor growth. *Proc Natl Acad Sci USA* **110:**14676–14681.

Song J, Oh JY, Sung YA, Pak YK, Park KS, and Lee HK (2001) Peripheral blood mitochondrial DNA content is related to insulin sensitivity in offspring of type 2 diabetic patients. *Diabetes Care* **24:**865–869.

Spinazzi M, Casarin A, Pertegato V, Salviati L, and Angelini C (2012) Assessment of mitochondrial respiratory chain enzymatic activities on tissues and cultured cells. *Nat Protoc* **7:**1235–1246.

Suzuki A, Yasuno T, Kojo H, Hirosumi J, Mutoh S, and Notsu Y (2000) Alteration in expression profiles of a series of diabetes-related genes in db/db mice following treatment with thiazolidinediones. *Jpn J Pharmacol* **84:**113–123.

Tang WH and Maroo A (2007) PPARgamma agonists: safety issues in heart failure. *Diabetes Obes Metab* **9:**447–454.

Turner N, Bruce CR, Beale SM, Hoehn KL, So T, Rolph MS, and Cooney GJ (2007) Excess lipid availability increases mitochondrial fatty acid oxidative capacity in muscle: evidence against a role for reduced fatty acid oxidation in lipid-induced insulin resistance in rodents. *Diabetes* **56:**2085–2092.

Wiley SE, Murphy AN, Ross SA, van der Geer P, and Dixon JE (2007) MitoNEET is an iron-containing outer mitochondrial membrane protein that regulates oxidative capacity. *Proc Natl Acad Sci USA* **104:**5318–5323.

Zuris JA, Harir Y, Conlan AR, Shvartsman M, Michaeli D, Tamir S, Paddock ML, Onuchic JN, Mittler R, Cabantchik ZI, et al. (2011) Facile transfer of [2Fe-2S] clusters from the diabetes drug target mitoNEET to an apo-acceptor protein. *Proc Natl Acad Sci USA* **108:**13047–13052.

**Address correspondence to:** Takehiro Takahashi, Pharmaceutical Research Laboratories, Toray Industries, Inc., 10-1, Tebiro 6-chome, Kamakura, Kanagawa 248-8555, Japan. E-mail: Takehiro_Takahashi@nts.toray.co.jp